17th June 2019

RE: Submission of revised manuscript cp-2019-25

Dear Prof. Zhengtang Guo,

Please, find our point by point reply to the reviewers' comments below along with the manuscript with tracked changes.

We thank the reviewers for their comments, which we believe helped strengthen this study. In addition to their suggestions, we have done the following changes to the manuscript:

- We have incorporated the available aragonite speleothems into our analyses. A detailed explanation about how we have converted them to their drip-water equivalent is in lines 210-234 (section 2.3). Because of this change, we have revised all figures and tables.

- We have removed the Multivariate Analyses from the Supplementary Material and instead added one new figure (Figure S1) and two new tables (Table S1 and S2), which complement Figures S5 and S6.

- We have corrected for typos and revised sentences that were not clear.

All the changes done to the manuscript can be found after our point-by-point answers to the reviewers, with the changes are shown in red.

We hope that the revised manuscript satisfies both the reviewers and the yourself.

Many thanks for taking your time to deal with our manuscript. Please, do not hesitate to contact me with further questions or requests.

Best regards,

Laia Comas Bru

Post-doctoral researcher
University of Reading, UK

Please note that the reviewer's comments are in black and our answers in blue.

Reply to anonymous Referee #1

1 Major comment: what is the added value of looking at spatial patterns for past climates compared to looking at them for present-day?

The authors argue that it is useful for model evaluation to look at spatial patterns of absolute δ 18O for past climates (LGM, MH) rather than just looking at anomaly maps, in contrast with many previous studies. This allows to have more sites for modeldata comparison. However, what is the added value of looking at spatial patterns for past climates compared to looking at them for present-day? For present-day, spatial patterns would be the same to first order. At present, there are so many more sites available directly samplig precipitation (GNIP), so why bother with speleothem records for past climates?

Figures 7 and 8 show the spatial patterns of observed and simulated δ 18O for LGM and MH. The sub-figure a representing North and South America are common to both figures, and they actually show very similar patterns. The same figure for present day would also show very similar patterns. This is because δ18O, temperature or precipitation changes between LGM, MH and present-day are much smaller than the magnitude of spatial variations along a transect covering such a wide range of latitudes. So these figures support my skepticism about the relevance of spatial patterns in absolute values for past climates. Figures 7b,c and 8b,c do not represent the same regions. But I'm sure that the maps for present-day would look very similar.

The corresponding text bears several slips of the pen and/or interpretation errors, that probably reflect that writing this sub-section was not confortable:

– l 408: "δ18O changes" should be replaced by "δ18O patterns": the authors write "changes" because this is really what is interesting to look at, but actually the figures do not show it.

– l 412: "underestimates changes in precipitation": again, we cannot see changes from present-day to MH on this figure.

What you want to plot depends on the science question. If the science question is what controls spatial patterns in absolute values, then it's better to focus on present day values; past climates do not provide much added value. But if the science question is what controls the changes at paleo-climatic time scales, then it is necessary to look at anomalies between 2 climatic states.

So I recommend to remove section 3.4, or replace it by an analysis of spatial patterns of anomalies, and to modify accordingly the abstract, protocol and conclusions.

We have removed the old Figures 7 and 8 and substitute them for two new figures showing the spatial patterns across time-periods (i.e., modern, MH and LGM) across Europe and Asia. These new figures show that the gradients change over time due to the large ice-sheets during the LGM and the different insolation patterns at different latitudes during the MH. We use these figures to illustrate how the model is not able to simulate these gradients in some cases.

We have also decided to focus only on isotope data and have therefore removed the pollen-based reconstructions completely.

Please see the revised section 3.4 in lines 447-481.

{2 Detailed comments

L157-158: I don't understand what this means. Where is the control simulations included in the LGM-MH difference?

We have clarified this in the text with the following sentence (see lines 161-165):

"We also calculated the anomaly between the LGM and MH (LGM-MH), taking account of the difference between their control simulations in the following way: (lgm_{PI}-lgm) – ($6ka_{PI}$-6ka)."

L209: remove "non-equilibrium of"

We have done this (see lines 220-221)

L216: add a dot.

We have done this

L223: remove "with data ... baseline".

We have clarified this sentence by writing (see lines 239-241):

"Data-model comparisons are generally made by comparing (1) anomalies between a control period and a palaeoclimate simulation with (2) data anomalies with respect to a modern baseline."

L234-235: already said, remove.

We agree with the reviewer that this has already been mentioned in L156-158 and the text has been deleted.

246: define pchip

We have added the definition of pchip: "piecewise cubic hermite interpolation" in the text (see line 260)

L295: clarify the rationale. Why can't there be a sampling bias in temperate regions towards the PMIP periods?

The previous sentence already suggested that the deviations could result from a sampling bias. However, we have rephrased this sentence to clarify this point (see lines 316-321)):

"These deviations could arise from sampling biases but it is unlikely that such biases would lead to differences between the tropics and temperate regions. Differences between curves constructed for both tropical and temperate regions (Fig. 2 c) suggest that, at least for the last 130 ka, deviations from expected stalagmite growth in the extra-tropics correspond to variability on glacial/interglacial scales."

L296: clarify this sentence. What does "even at a global level" mean?

We have deleted this sentence and replaced it by (see lines 323-326):

"Thus, the speleothem data indicate similar climatic sensitivity, even at a global level, to that demonstrated for sub-continental and regional scales by earlier authors, despite their use of much smaller numbers and far less precise age data than in the SISAL dataset."

L300-302: can you explain briefly why higher latitude speleothems are more depleted than OIPC and low latitude speleothems are more enriched?

This comment is not relevant any more. The scatterplots in figure 3 were updated after incorporating aragonite speleothems in this study. The text describing the revised figure is in line 333.

L305:"cave specific factors" cannot explain why you have such systematic differences common to wide regions.

We refer to our answer above.

L317-319: should the reader conclude that ECHAM underestimates the interannual variability? If so, please state this clearly. Has such a bias already been described in a previous paper, for ECHAM or for other models? Explain briefly what could be the reason for this underestimate.

We have modified the manuscript to incorporate information on why ECHAM is underestimating d18O variability (see lines 358-363):

"Our results are consistent with the general tendency of climate models to underestimate the sensitivity of extreme precipitation to temperature variability or trends (Flato et al., 2014). ECHAM5 is known to underestimate inter-annual variability in regions where precipitation is dominantly convective (i.e., the tropics), as well as in summer in extra-tropical regions (e.g., in southern Europe) because convective precipitation operates on small spatial scales and has a large random component, even for a given large-scale atmospheric state (Eden et al., 2012)."

L321: move "processes" before "within"

We have revised this sentence to read (see line 365):

"… reflecting the impact of karst and in-cave processes that effectively act as a low-pass filter..."

L325-328: this has already been said just above.

We have now deleted the duplicated part of that sentence (see lines 369-372).

L359: replace "anomalies" by "MH values"?

We have made the suggested change in the text. See line 404.

L422: remove "utilising"

We have rephrased this sentence to (see line 483-484)

"Our analyses illustrate a number of possible approaches for using speleothem isotopic data for model evaluation."

L440-447: this issue was not previously discussed. Add some quantification, or a map, showing what error we would make if we use only the fractionation factor for calcite?

While the impact of using one of another fractionation equation is minimal (i.e. smaller than the measurement uncertainty) for sites with MAT > 27.3C, the added uncertainty is noticeable at sites with lower MAT. Changes of MAT across time periods could exacerbate these differences for individual sites thus making the calculated entity-based anomalies inaccurate. As requested by the reviewer, we have now added new supplementary figure (Fig. S1) to show that using the appropriate correction according to the speleothem's mineralogy is important.

L473: remove "on a global basis". Or clarify what you mean. Even at a specific cave, if the speleothem acts as a low pass filter, time scales shorter than "quasidecadal" cannot be studied.

We have modified that last section of this paragraph to clarify this point (see lines 536-538):

The low variability shown by the SISAL records – most likely from the low-pass filter effectively applied to the speleothem record by the karst system – precludes the use of this database for global studies focused on time scales shorter than quasi-decadal."

In addition, we have also added the following text in the results section 3.2 to clarify this point (see lines 372-375):

"This result indicates that global data-model comparisons using speleothem records should focus on quasi-decadal or longer timescales. However, the temporal smoothing caused by karst processes varies from site to site; where transmission from the surface to the cave can be shown to be rapid, individual speleothems may preserve annual or even sub-annual signals."

L475-476: clarify. Do you mean that the model underestimates δ18O changes?

Yes, the model underestimates the amplitude of $\delta^{18}O$ changes as recorded in the speleothems. For details we refer the reviewer to our answers on their comment on L317-319. We have rephrased this sentence to (see lines 540-543):

"Using the traditional anomaly approach to data-model comparisons, there is consistency between the sign of observed and simulated changes in both the MH and the LGM exists. However, the ECHAM5-wiso model underestimates the changes in $\delta_{18}O$ between time periods compared to the speleothems records (i.e., the amplitude of modelled $\delta_{18}O$ changes is lower)."

L476-477: clarify.

We agree that this sentence is too broad and general and have decided to delete it.

L489: "constraining structural error on the model side": what do you mean? There are plenty of sources of errors in the model: errors on forcings, missing processes in parameterization package, tunable parameters, coarse resolution... Which one are you refering to? "true uncertainties": beware that errors are not the same as uncertainties. Anyway, in this paragraph, I suggest to focus only on uncertainties on the observation side, because this is what is useful to evaluate models. The question of quantifying uncertainties in models is set differently and is beyond the scope of this paper.

We have rephrased this sentence to (see lines 506-515):

"Mismatches between simulations and observations can reflect the issues with the experimental design, problems with the model or uncertainties in the observations (Harrison et al., 2015). The failure to include changes in atmospheric dust loading, for example, has been put forward as an explanation of data-model mismatches in both the MH and the LGM (e.g., Hopcroft et al., 2015; Messori et al., 2019). Missing processes and feedbacks, such as climate-induced vegetation or land-surface changes, could also contribute to mismatches (e.g., Yoshimori et al., 2009; Swann et al., 2014). Uncertainties caused by the specific structure of the model or assigned model parameter values could also contribute to data-model mismatches (Qian et al., 2016). Ultimately, there needs to be an assessment of the contribution of all of these factors to data-model mismatches, but here we have only focused on potential uncertainties associated with the speleothem data."

Reply to Anonymous Referee #2

Minor issues

Are the control runs for MH and LGM different? Probably I don't catch the points. In my understanding, they should be the same which is the base for probing the climatic significance of the difference between the MH and LGM simulation experiments.

As suggested by reviewer 1, we have clarified how we have taken into account the difference in control runs for the MH and LGM simulations with the following sentence (see lines 161-165):

"We also calculated the anomaly between the LGM and MH (LGM-MH), taking account of the difference between their control simulations in the following way: (lgm_{PI}-lgm) – ($6ka_{PI}$-6ka)."

The simulation results of the MH seem to be better than that of the LGM. Could they explain more on this? For example, they use the protocol of PIMP3 for the LGM modelling, and their SST forcing is based on the results of a full transient experiment. More clarification on why they take such steps will make this manuscript more convinced.

Unfortunately, we cannot say that the MH simulation results fit better to the speleothem data compared to the LGM simulation due to the limited number of speleothem records available during the LGM.

Reply to Anonymous Referee #3

I don't see very well what is the advancement made by this study as compared to the traditional approach for comparing the speleothem records with models. Maybe the authors should stress more why their approaches are better and what new can been discovered by their approaches that cannot be done by traditional approach.

Data-model comparisons using speleothem data are comparatively new and have tended to focus on validation of new versions of isotope-enabled models. These comparisons have often overlooked important characteristics of, and/or uncertainties associated with, the speleothem records (see discussion section). There is no agreed protocol for using speleothem data for model evaluation. The purpose of our paper is to identify issues that could affect data-model comparisons, drawing on the new SISAL database that has been explicitly constructed to facilitate such comparisons and the expertise of the speleothem experts who constructed this database. Thus, we are not claiming that our approach is different from or better than a "traditional" approach – we are simply making it clear how speleothem data should and could be used. We have clarified the purpose of the paper by amplifying our description in L107-111 as follows:

"In this paper, we examine a number of issues that need to be addressed in order to use speleothem data, specifically data from the SISAL database, for model evaluation in the palaeoclimate context and make recommendations about robust approaches that should be used for model evaluation in CMIP6-PMIP4. We focus particularly on interpretation issues that could be overlooked in using 110 speleothem records and we show the strengths and limitations of different comparison techniques."

In addition, we have also expanded the conclusion section (see lines 582-594) to better clarify the purpose of this paper. Here we refer to the answer below.

It is not very clear to me what is the final goal of the data-model comparison and what can be improved or learned after all the analyses. If the comparison is good, can we assume that the temperature and precipitation simulated by the model are correct and what is the uncertainty? What might be the reasons for the similarities and differences between model results and speleothem data? Can the results help to improve the model and/or experiment design and how?

As explained in the introduction (lines 41-53), model evaluation using palaeoclimate data provides an out-of-sample test of model performance and is one component of the Palaeoclimate Modelling Intercomparison Project. Such evaluations help to provide confidence in the projections of future climates. Speleothems are a relatively new source of information for such evaluations and the purpose of our paper is to provide a robust framework to make such evaluations. We do not want to distract from this goal by discussing the generic purposes of data-model comparison in the Introduction to the paper, but we have added a concluding paragraph discussing what can be learnt from such data-model comparisons as follows (L582-594):

"Comparisons with speleothem data can be seen as a complement to model evaluation using other types of palaeoenvironmental data and palaeoclimatic reconstructions (see e.g. MARGO Project Members, 2009; Harrison et al., 2014). They can be considered particularly useful because they provide insights into how well state-of-the-art models reproduce the hydrological cycle and atmospheric circulation patterns. The ability to reproduce past observations provides additional confidence in the ability of climate models to simulate large climate changes, such as those expected by the end of the 21st century (Braconnot et al., 2012; Schmidt et al., 2014). However, mismatches between model simulations and palaeo-observations are also useful because they can help to pinpoint issues that may need to be addressed in developing improved models or in better experimental protocols (Kageyama et al., 2018), providing that these mismatches do not arise because of misunderstanding or misinterpretation of the observations themselves. By providing a protocol for using speleothem data for data-model comparisons that accounts for uncertainties in the observations, we anticipate that at least such causes of data-model mismatches will be minimized."

The major uncertainties and biases of the ECHAM5-wiso model in simulating present day and past climates and the experiment design of the MH and LGM simulations, the reliability of the SST and sea ice simulated by the CCSM3 and their potential influence on the data-model comparison should be discussed.

We use outputs from the ECHAM-wiso model in order to illustrate potential approaches to data-model comparison. Our goal here is not to provide an in-depth evaluation of the quality of these simulations. The performance of the ECHAM-wiso model under modern day conditions has been extensively analysed (see e.g. Werner et al., 2011; Wackerbarth et al., 2012) and the MH and LGM simulations have also been published and discussed (Wackerbarth et al., 2012; Werner et al., 2018). In order to make it clear that our use of the model is illustrative, we have revised the final section of the introduction to read:

"We use an updated version of the SISAL database (SISALv1b: Atsawawaranunt et al., 2019) and simulations made with the ECHAM5-wiso isotope-enabled atmospheric circulation model (Werner et al., 2011) to explore the various issues in making data-model comparisons. The goal is not to evaluate the ECHAM5-wiso simulations but rather to use them to illustrate generic issues in data-model comparison with speleothem isotopic data."

The simulations for MH and LGM are only 12 and 22 years. Are they long enough to allow the climate at different speleothem location reaching equilibrium? What is the initial state of these simulations? What might be the influence of using fixed ocean condition?

We explain in the methods section (lines 133-164) that these simulations are atmosphere-only simulations forced with sea-surface temperatures and sea-ice cover from a pre-existing transient simulation. Thus, there is no spin-up necessary and the issue of equilibrium is irrelevant. If the purpose of this paper were to use the model simulations to explain speleothem records, then the lack of ocean coupling would mean that the simulations would be unsuitable for evaluating the degree to which long-term (multi-decadal) variability in the speleothem isotope record reflected internal unforced variability. But as our purpose in using the experiments is illustrative, then the short length of the simulations is not important. We hope that the modification to the introduction mentioned above will help clarify the purpose of this paper.

Evaluating model outputs using integrated global speleothem records of climate change since the last glacial

Laia Comas-Bru[1,2], Sandy P. Harrison[1], Martin Werner[3], Kira Rehfeld[4], Nick Scroxton[5], Cristina Veiga-Pires[6] and SISAL working group members

[1]School of Archaeology, Geography & Environmental Sciences, Reading University, Whiteknights, Reading, RG6 6AH, UK
[2]UCD School of Earth Sciences. University College Dublin, Belfield. Dublin 4, Ireland.
[3]Alfred Wegener Institute. Helmholtz Centre for Polar and Marine Research. Division Climate Science - Paleoclimate Dynamics. Bussestr. 24, D-27570 Bremerhaven, Germany
[4]Institute of Environmental Physics, Ruprecht-Karls-Universität Heidelberg, Im Neuenheimer Feld 229, 69120 Heidelberg, Germany
[5]Department of Geosciences, University of Massachusetts Amherst, 611 North Pleasant Street, 01003-9297 Amherst, MA, USA
[6]Universidade do Algarve Faculdade de Ciências do Mar e do Ambiente - FCMA Centro de Investigação Marinha e Ambiental - CIMA Campus de Gambelas 8005-139 Faro Portugal

Correspondence to: Laia Comas-Bru (l.comasbru@reading.ac.uk)

Abstract: Although quantitative isotopic data from speleothems has been used to evaluate isotope-enabled model simulations, currently no consensus exists regarding the most appropriate methodology through which to achieve this. A number of modelling groups will be running isotope-enabled palaeoclimate simulations in the framework of the Coupled Model Intercomparison Project Phase 6, so it is timely to evaluate different approaches to use the speleothem data for data-model comparisons. Here, we ~~accomplish~~ illustrate this using 456 globally-distributed speleothem $\delta^{18}O$ records from an updated version of the Speleothem Isotopes Synthesis and Analysis (SISAL) database and palaeoclimate simulations generated using the ECHAM5-wiso isotope-enabled atmospheric circulation model. We show that the SISAL records reproduce the first-order spatial patterns of isotopic variability in the modern day, strongly supporting the application of this dataset for evaluating model-derived isotope variability into the past. However, the discontinuous nature of many speleothem records complicates procuring large numbers of records if data-model comparisons are made using the traditional approach of comparing anomalies between a control period and a given palaeoclimate experiment. To circumvent this issue, we illustrate techniques through which the absolute isotopic values during any time period could be used for model evaluation. Specifically, we show that speleothem isotope records allow an assessment of a model's ability to simulate spatial isotopic trends ~~and the degree to which the model reproduces the observed environmental controls of isotopic spatial variability~~. Our analyses provide a protocol for using speleothem isotopic data for model evaluation, including screening the observations to take into account the impact of speleothem mineralogy on $\delta^{18}O$ values, the optimum period for the modern observational baseline, and the selection of an appropriate time-window for creating means of the isotope data for palaeo time slices.

1 Introduction

Earth System Models (ESMs) are routinely used to project the consequences of current and future anthropogenic forcing of climate, and the impacts of these projected changes on environmental services (e.g., Christensen et al., 2013; Collins et al., 2013; Kirtman et al., 2013; Field, 2014). ESMs are routinely evaluated using modern and historical climate data. However, the range of climate variability experienced during the period for which we have reliable historic climate observations is small, much smaller than the amplitude of changes projected for the 21st century. Radically different climate states in the geologic past provide an opportunity to test the performance of ESMs in response to very large changes in forcing, changes that in some cases are as large as the expected change in forcing at the end of the 21st century (Braconnot et al., 2012). The use of "out-of-sample" testing (Schmidt et al., 2014) is now part of the evaluation procedure of the Coupled Model Intercomparison Project (CMIP). Several palaeoclimate simulations are being run by the Palaeoclimate Modelling Intercomparison Project (PMIP) as part of the sixth phase of CMIP (CMIP6-PMIP4), including simulations of the Last Millennium (LM, 850–1850 CE, *past1000*), mid-Holocene (MH, ca. 6,000 yrs BP, *midHolocene*) Last Glacial Maximum (LGM, ca. 21,000 yrs BP, *lgm*), the Last Interglacial (LIG, ca. 127,000 yrs BP, *lig127k*) and the mid-Pliocene Warm Period (mPWP, ca. 3.2 M yrs BP, *midPliocene-eoi400*) (Kageyama et al., 2017).

Although these CMIP6-PMIP4 time periods were selected because they represent a range of different climate states, the choice also reflects the fact that global syntheses of palaeoenvironmental and palaeoclimate observations exist across them, thereby providing the opportunity for model benchmarking (Kageyama et al., 2017). However, both the geographic and temporal coverage of the different types of data is uneven. Ice core records are confined to polar and high-altitude regions and provide regionally to globally integrated signals of forcings and climatic responses. Marine records provide a relatively comprehensive coverage of the ocean state for the LGM, but low rates of sedimentation mean they are less informative about the more recent past (Hessler et al., 2014). Lake records provide qualitative information of terrestrial hydroclimate, but the most comprehensive source of quantitative climate information over the continents is based on statistical calibration of pollen records (see e.g., Bartlein et al., 2011). However, pollen preservation requires the long-term accumulation of sediments under anoxic conditions and is consequently limited in semi-arid, arid and highly dynamic wet regions such as in the tropics.

Oxygen isotopic records ($\delta^{18}O$) from speleothems, secondary carbonate deposits that form in caves from water that percolates through carbonate bedrock (Hendy and Wilson, 1968; Atkinson et al., 1978; Fairchild and Baker, 2012), provide an alternative source of information about past terrestrial

climates. Although there are hydroclimatic limits on the growth of speleothems, their distribution is largely constrained by the existence of suitable geological formations and they are found growing under a wide range of climate conditions, from extremely cold climates in Siberia (Vaks et al., 2013) to arid regions of Australia (Treble et al., 2017). Therefore, speleothems have the potential to provide information about past terrestrial climates in regions for which we do not have (and are unlikely to have) information from pollen. As is the case with pollen, where quantitative climate reconstructions must be obtained through statistical or forward modelling approaches (Bartlein et al., 2011), the interpretation of speleothem isotope records in terms of climate variables is in some cases not straightforward (Lachniet, 2009; Fairchild and Baker, 2012). However, some ESMs now use water isotopes as tracers for the diagnosis of hydroclimate (Schmidt et al., 2007; Tindall et al., 2009; Werner et al., 2016), and this opens up the possibility of using speleothem isotopic measurements directly for comparison with model outputs. At least six modelling groups are planning isotope-enabled palaeoclimate simulations as part of CMIP6-PMIP4.

As with other model evaluation studies, much of the diagnosis of isotope-enabled ESMs has focused on modern day conditions (e.g., Joussaume et al., 1984; Hoffmann et al., 1998; Hoffmann et al., 2000; Jouzel et al., 2000; Noone and Simmonds, 2002; Schmidt et al., 2007; Roche, 2013; Xi, 2014; Risi et al., 2016; Hu et al., 2018). However, isotope-enabled models have also been used in a palaeoclimate context (e.g., Schmidt et al., 2007; LeGrande and Schmidt, 2008; LeGrande and Schmidt, 2009; Langebroek et al., 2011; Caley and Roche, 2013; Caley et al., 2014; Jasechko et al., 2015; Werner et al., 2016; Zhu et al., 2017). The evaluation of these simulations has often focused on isotope records from polar ice cores and from marine environments. Where use has been made of speleothem records, the comparison has generally been based on a relatively small number of the available records. Furthermore, all of the comparisons make use of an empirically-derived correction for the temperature-dependence fractionation of calcite $\delta^{18}O$ at the time of speleothem formation that is based on synthetic carbonates (Kim and O'Neil, 1997). This fractionation is generally poorly constrained (McDermott, 2004; Fairchild and Baker, 2012), does not account for any non-equilibrium of kinetic fractionation at the time of deposition and is not suitable for aragonite samples. Thus, using a single standard correction and not screening records for mineralogy introduces uncertainty into the data-model comparisons.

SISAL (Speleothem Isotopes Synthesis and Analysis), an international working group under the auspices of the Past Global Changes (PAGES) project (http://pastglobalchanges.org/sisal), is an initiative to provide a reliable, well-documented and comprehensive synthesis of isotopic records from speleothems worldwide (Comas-Bru and Harrison, 2019). The first version of the SISAL database

(SISALv1: Atsawawaranunt et al., 2018a; Atsawawaranunt et al., 2018b) included 381 speleothem-based isotope records and metadata to facilitate quality control and record selection. A major motivation for the SISAL database was to provide a tool for benchmarking of palaeoclimate simulations using isotope-enabled models.

In this paper, we examine a number of issues that need to be addressed in order to use speleothem data, specifically data from the SISAL database, for model evaluation in the palaeoclimate context and make recommendations about robust approaches that should be used for model evaluation in CMIP6-PMIP4. We focus particularly on interpretation issues that could be overlooked in using speleothem records and we show the strengths and limitations of different comparison techniques. We use ~~on~~ the MH and LGM time periods, partly because the *midHolocene* and *lgm* experiments are the "entry cards" for the CMIP6-PMIP4 simulations and partly because these are the PMIP time periods with the best coverage of speleothem records. We use an updated version of the SISAL database (SISALv1b: Atsawawaranunt et al., 2019) and simulations made with the ECHAM5-wiso isotope-enabled atmospheric circulation model (Werner et al., 2011) to explore the various issues in making data-model comparisons. Our goal is not to evaluate the ECHAM5-wiso simulations but rather to use them to illustrate generic issues in data-model comparison with speleothem isotopic data.

Section 2 introduces the data and the methods used in this study. Section 2.1 introduces the isotope-enabled model simulations for the modern (1958–2013), the *midHolocene* and the *lgm* experiments, explains the methods used to calculate weighted simulated $\delta^{18}O$ values, and provides information about the construction of time-slices. Section 2.2 presents the modern observed $\delta^{18}O$ in precipitation ($\delta^{18}O_p$) used. Section 2.3 introduces the speleothem isotopic data from the SISAL database and explains the rationale for screening records. Section 3 describes the results of the analyses, specifically the spatio-temporal coverage of the SISAL records (Section 3.1), the representation of modern conditions (Section 3.2), anomaly-mode time-slice comparisons (Section 3.3), and the comparison of $\delta^{18}O$ gradients in absolute values along spatial transects to test whether the model accurately records ~~regional~~ latitudinal variations in $\delta^{18}O$ across time periods (Section 3.4). Section 4 provides a protocol for using speleothem isotopic records for data-model comparisons and section 5 summarises our main conclusions.

2 Methods

2.2 Model simulations

ECHAM5-wiso (Werner et al., 2011; Werner, 2019) is the isotope-enabled version of the ECHAM5 Aatmosphere Global Circulation Model (Roeckner et al., 2003; Hagemann et al., 2006; Roeckner et al.,

2006). The water cycle in ECHAM5 contains formulations for evapotranspiration of terrestrial water, evaporation of ocean water, and the formation of large-scale and convective clouds. Vapour, liquid, and frozen water are transported independently within the atmospheric advection scheme. The stable water isotope module in ECHAM5 computes the isotopic signal of different water masses through the entire water cycle, including in precipitation and soil water.

ECHAM5-wiso was run for 1958–2013~~,~~ using an implicit nudging technique to constrain simulated fields of surface pressure, temperature, divergence and vorticity to the corresponding ERA-40 and ERA-Interim reanalysis fields (Butzin et al., 2014). The *midHolocene* simulation (Wackerbarth et al., 2012) was forced by orbital parameters and greenhouse gas concentrations appropriate to 6 ka following the PMIP3 protocol (https://pmip3.lsce.ipsl.fr). The control simulation has modern values for the orbital parameters and greenhouse gas (GHG) concentrations (Wackerbarth et al., 2012). The change in sea surface temperatures (SST) and sea ice cover between 6 ka and the pre-industrial period were calculated from 50-year averages from each interval extracted from a transient Holocene simulation performed with the fully coupled ocean-atmosphere Community Climate System Model ~~CCSM3~~ (CCSM3; Collins et al., 2006). The anomalies were then added to the observed modern SST and sea ice cover data to force the *midHolocene* simulation (Wackerbarth et al., 2012). For the *lgm* experiment (Werner et al., 2018), orbital parameters, GHG concentrations, land-sea distribution, and ice sheet height and extent followed the PMIP3 guidelines. Climatological monthly sea ice coverage and SST changes were prescribed from the GLAMAP dataset (Paul and Schäfer-Neth, 2003). A uniform glacial enrichment of sea surface water and sea ice of +1‰ ($\delta^{18}O$) and +8‰ (δD) on top of the present-day isotopic composition of surface seawater was applied. For the ocean surface state of the corresponding control simulation, monthly climatological SST and sea ice cover for the period 1979-1999 were prescribed. All the ECHAM5-wiso simulations were run at T106 horizontal grid resolution (approx. 1.1°x1.1°) with 31 vertical levels. The *midHolocene* and *lgm* experiments were run for 12 and 22 years, respectively, and the last 10 (*midHolocene*) and 20 (*lgm*) years were used to construct the anomalies. Model anomalies for the MH and the LGM were calculated as the differences between the averaged *midHolocene*/*lgm*~~MH/LGM~~ simulations and their corresponding control~~ simulations~~. We also calculated the anomaly between ~~the~~ *lgm*~~LGM~~ and *midHolocene*~~MH (LGM-MH)~~, taking account of the difference between their control simulations~~.~~ in the following way: (*lgm* - lgm_{PI}) - (*midHolocene* - $midHolocene_{PI}$).~~We constructed simulated isotope anomalies by averaging the last 10 (*midHolocene*) and 20 (*lgm*) years of the simulations.~~

At best, the speleothem isotopic signal will be an average of the precipitation $\delta^{18}O$ ($\delta^{18}O_p$) signals weighted towards those months when precipitation is greatest (Yonge et al., 1985). However, the

signal is transmitted via the karst system, and is therefore modulated by storage in the soil, recharge rates, mixing in the subsurface, and varying residence times - ranging from hours to years (e.g., Breitenbach et al., 2015; Riechelmann et al., 2017). These factors could all exacerbate differences between observations and simulations. We investigated whether weighting the simulated $\delta^{18}O$ signals by soil moisture or recharge amount provided a better global comparison ~~measure~~ than weighting by precipitation amount by calculating three indices: (i) $\delta^{18}O_p$ weighted according to monthly precipitation amount ($w\delta^{18}O_p$); (ii) $\delta^{18}O_p$ weighted according to the potential recharge amount calculated as precipitation minus evaporation (P-E) for months where P-E > 0 ($w\delta^{18}O_{recharge}$); and (iii) soil water $\delta^{18}O$ weighted according to soil moisture amount ($w\delta^{18}O_{sw}$). To investigate the impact of transit time on the comparisons, we smoothed the simulated $w\delta^{18}O$ using a range of smoothing from 1–16~~20~~ years. Finally, we investigated whether differences in elevation between the model grid and speleothem records had an influence on the quality of the data-model comparisons by applying an elevational correction of -2.5‰/km (Lachniet, 2009) to the simulated $w\delta^{18}O$.

2.2 Modern observations

We use two sources of modern isotope data for assessment purposes: (i) $\delta^{18}O_p$ measurements from the Global Network of Isotopes in Precipitation (GNIP) database (IAEA/WMO, 2018) and (ii) a gridded dataset of global water isotopes from the Online Isotopes in Precipitation Calculator (OIPC: Bowen and Revenaugh, 2003; Bowen, 2018).

The GNIP database (IAEA/WMO, 2018) provides raw monthly $\delta^{18}O_p$ values for some part of the interval 03/1960 to 08/2017 for 977 stations. Individual stations have data for different periods of time and there are gaps in most individual records; only two stations have continuous data for over 50 years and both are in Europe (Valentia Observatory, Ireland, and Vienna Hohe-Warte, Austria). Most GNIP stations are more than 0.5° away from the SISAL cave sites, precluding a direct global comparison between GNIP and SISAL records. However, the GNIP data can be used to examine simulated interannual variability. Annual $w\delta^{18}O$ averages were calculated from GNIP stations with ~~at least~~enough ~~10~~ months of data to account for more than 80% of the annual precipitation ~~per year~~ and 5 or more years of data. Annual $w\delta^{18}O_p$ data was extracted from the ECHAM5-wiso simulations at the location of the GNIP stations for the years for which GNIP data is available at each station. We exclude GNIP stations from coastal locations that are not land in the ECHAM5-wiso simulation. This dual screening results in only 450 of the 977 GNIP stations being used for comparisons. Boxplots are calculated with the standard deviation of annual $w\delta^{18}O_p$ data.

The OIPC dataset provides a gridded long-term ~~global~~ (1960–2017) global record of modern $w\delta^{18}O_p$, based on combining data from 348 GNIP stations covering part or all the period 1960–2014 (IAEA/WMO, 2017) and other $w\delta^{18}O_p$ records from the Water Isotopes Database (Waterisotopes Database, 2017). The OIPC data can be used to evaluate modern spatial patterns in both the SISAL records and the simulations.

2.3 Speleothem isotope data

We use an updated SISAL database (SISALv1b: Atsawawaranunt et al., 2019), which provides revised versions of 45 records from SISALv1 and includes 60 new records (Table 1). SISALv1b has isotope records from 455 speleothems from 211 cave sites distributed worldwide. Because the isotopic fractionation between water and $CaCO_3$ differs between calcite and aragonite, ~~-~~we ~~only~~ use calcite speleothems, ~~or~~ aragonite speleothems where the correction to calcite values was made by the original authors, and ~~for simplicity~~ speleothems with uncorrected aragonite mineralogy. ~~However, using the reformulated aragonite $\delta^{18}O$ water equation of Grossman and Ku (1986) from Lachniet (2015) would allow the incorporation of the currently small number of aragonite records from the SISAL database to the data-model comparison.~~ We exclude speleothems where some samples are calcite and some aragonite (mixed mineralogy speleothems) and speleothems with unknown mineralogy. As a result of this screening, we use ~~370~~ 407 speleothem records from ~~174~~ 193 cave sites for comparisons. However, the number of speleothem records covering specific periods (i.e., modern, MH, LGM) is considerably lower.

Recent data suggests that many calcite speleothems are precipitated out of isotopic equilibrium with waters (Daëron et al., 2019). Therefore, we have converted ~~SISAL~~ speleothem calcite data to its drip-water equivalent using an empirical speleothem-based fractionation factor that accounts for any ~~non-equilibrium of~~ kinetic fractionation that may arise in the precipitation of calcite speleothems in caves (Tremaine et al., 2011):

$$\delta^{18}O_{dripw\_SMOW} = \delta^{18}O_{calcite\_SMOW} - \left(\left(\frac{16.1 \cdot 1000}{T}\right) - 24.6\right) \quad \text{(T in K)}$$

We use the fractionation factor from Grossman and Ku (1986) as formulated in Lachniet (2015) to convert aragonite speleothems to their drip-water equivalent:

$$\delta^{18}O_{dripw\_SMOW} = \delta^{18}O_{calcite\_SMOW} - \left(\left(\frac{18.34 \cdot 1000}{T}\right) - 31.954\right) \quad \text{(T in K)}$$

We use the V-PDB to V-SMOW conversion from Coplen et al. (1983) as in Sharp (2007):

$$\delta^{18}O_{calcite\_SMOW} = 1.03092\text{~~0.97002 ·~~ x } \delta^{18}O_{calcite\_PDB} + 30.92\text{~~29.98~~}$$

We have used mean annual surface air temperature from CRU-TS4.01 (Harris et al., 2014) for the OIPC comparison and ECHAM5-wiso simulated mean annual temperature for the SISAL-model comparison as a surrogate ~~of~~ for modern and past cave air temperature (Moore and Sullivan, 1997). There are u~~U~~ncertainties ~~are introduced~~ in this conversion ~~from~~ because several ~~unknown~~ factors are unknown, e.g., ~~such as~~ cave temperature and pCO_2 of soil.

We compare the modern temporal variability in the SISAL records with ECHAM5-wiso by extracting simulated $w\delta^{18}O_p$ at the cave site location for all the years for which there are speleothem isotope samples within the period 1958-2013. The speleothem isotope ages were rounded to exact calendar years for this comparison.

Data-model comparisons are generally made by comparing (1) anomalies between a ~~control period and a~~ palaeoclimate simulation and a control period with (2) data anomalies with respect to a modern baseline. There is no agreed standard defining the interval used as a modern baseline for palaeoclimate reconstructions. Some studies have used modern observational datasets which cover a specific and limited period of time and some use the late 20th century as a reference. We investigate the appropriate choice of modern baseline for the speleothem records by comparing the interval centred on 1850 CE with alternative intervals covering the late 20th century, specifically 1961-1990 and 1850–1990 CE, and we assess the impact of these choices on both mean $\delta^{18}O$ values and the number of records available for comparison. The MH time slice was defined as 6,000 ±500 yrs BP (where present is 1950 CE) and the LGM time slice as 21,000 ±1,000 yrs BP, following the conventional definitions of these intervals used in the construction of other benchmark palaeoclimate datasets (e.g., MARGO project members, 2009; Bartlein et al., 2011). However, we also examined the impact of using shorter intervals for each time slice. ~~In addition to calculating LGM and MH anomalies with respect to modern, we also calculated the anomaly between the LGM and MH (LGM-MH).~~

We use the published age-depth models for each speleothem record. There is no information about the temporal uncertainties on individual isotope samples for most of the records in SISALv1b. This precludes a general assessment of the impact of temporal uncertainties on data-model comparisons. Nevertheless, w~~W~~e assess these impacts for the LGM for two records (entity BT-2 from Botuverá cave: Cruz et al., 2005; and entity SSC01 from Gunung-buda cave: Partin et al., 2007) for which new age-depth models have been prepared using COPRA (Breitenbach et al., 2012). We created 1,000-member ensembles of the age-depth relationship using the original author's choice of radiometric dates and

pchip (piecewise cubic hermite interpolating polynomial) interpolation. Isotope ratio means were calculated using time windows of increasing width (±100 to ~~3,000~~ ±1,500 years) around 21 kyrs BP for the original age-depth model, the COPRA median age model, and all ensemble members. All COPRA-based uncertainties have been projected to the chronological axes.

To explore the use of absolute isotopic data for model evaluation, we extracted absolute data for ~~six~~ two transects illustrating key features of the ~~MH and LGM~~ geographic isotopic patterns during the modern, MH and LGM periods. ~~The MH transects run from NW to SE across America, NW to SE across SE Asia, and N-S across southern Europe and northern Africa. The LGM transects run N-S from central Europe to southern Africa, from NW to SE in America, and N-S from China to northern Australia.~~ Each transect follows the great circle line between two locations. The ~~longitudinal~~ span of each regional transect varies to maximise the number of SISAL records included. We extracted model outputs for the same transects ~~,~~ at 1.12° steps to match the model grid size and using the model land/sea mask to remove ocean grid cells. ~~The simulated absolute values were extracted along the great circle lines at 1.12° steps to match the model grid size.~~ Comparisons are made between the SISAL mean $\delta^{18}O$ value and the simulated $w\delta^{18}O_p$ values averaged within ~~a~~ the latitudinal or longitudinal range defined for each transect. ~~We also compare simulated mean annual surface air temperature (MAT) and mean annual precipitation (MAP) with pollen-based quantitative reconstructions of MAT and MAP from Bartlein et al. (2011). The pollen-based anomalies have been converted to absolute values by adding the CRU TS4.01 climatology (Harris et al., 2014).~~

The presence/absence of speleothems in the temperate zone has long been interpreted as a direct indication of interstadial/stadial climate state (Gordon et al., 1989; Kashiwaya et al., 1991; Baker et al., 1993), while in dry regions speleothem growth indicates a pluvial climate (Vaks et al., 2006) and in episodically cold regions responds to the absence of permafrost (Atkinson et al., 1978; Vaks et al., 2013)~~Speleothem growth is inhibited in very dry climates, so the presence/absence of speleothems has been interpreted as a direct indication of climate state (Gascoyne et al., 1983;Vaks et al., 2006;Vaks et al., 2013)~~. Speleothem distribution through time approximates an exponential curve in many regions around the world (e.g., Ayliffe et al., 1998; Jo et al., 2014; Scroxton et al., 2016). This relationship suggests that the natural attrition of stalagmites is independent of the age of the specimens and approximately constant through time, despite potential complications from erosion, climatic changes and sampling bias. The underlying exponential curve can, therefore, be thought of as a prediction of the number of expected stalagmites given the existing population. Intervals when climate conditions were more/less favourable to speleothem growth can then be identified from changes in the population size by subtracting this underlying exponential curve (Scroxton et al., 2016).

We apply this approach at a global level to the unscreened SISAL data by counting the number of individual caves with stalagmite growth during every 1,000-yr period from 500 kyrs BP to the present. Growth was indicated by a stable isotope sample at any point in each 1,000-year bin, giving 3,866 data points distributed in 500 bins. We use cave numbers, rather than the number of individual speleothems, to minimise the risk of over-sampled caves influencing the results. Random resampling (100,000) of the 3,866 data points was used to derive 95% and 5% confidence intervals. The number of speleothems cannot be reliably predicted by a continuous distribution when numbers are low, so we do not consider intervals prior to 266 kyrs BP – the most recent interval with less than four records.

3 Results

3.1 Spatio-~~al and~~ temporal coverage of speleothem records

There are many regions of the world where the absence of carbonate lithologies means that there will never be speleothem records (Fig. 1a). Nevertheless, SISALv1b represents a substantial improvement in spatial coverage compared to SISALv1, particularly for Australasia and Central and North America~~n~~ (Fig. 1a, Table 1), and the sampling for regions such as Europe and China is quite dense. Thus, SISALv1b provides a sufficient coverage to allow the data to be used for model evaluation. The temporal distribution of records is uneven, with only ca. 40 at 21 kyrs increasing to > 100 records at 6 kyrs and > 110 for the last 1,000 yrs (Fig. 1b). A pronounced regional bias exists towards Europe during the Holocene. Regional coverage is relatively even during the LGM, with the exception of Africa which is under-represented throughout (< 4% of total). Nevertheless, there is sufficient coverage to facilitate data-model comparisons for the MH and LGM for most regions of the world.

The global occurrence of speleothems through time approximates an exponential distribution (Fig. 2 a~~, b~~). Anomalously high numbers of speleothems are found in the last 12 kyrs, between 128–112 kyrs BP and during interglacials MIS 1 and 5e (and the early glacial MIS 5d). There are fewer than expected speleothems between 73–63 kyrs BP and during MIS 2 (Fig. 2 b). These deviations could arise from sampling biases but ~~may also reflect globally wetter or drier intervals~~it is unlikely that such biases would lead to differences between the tropics and temperate regions. Differences between curves constructed for both tropical and temperate regions (Fig. 2 c~~, d~~) suggest that, at least for the last 130 ka, deviations from expected stalagmite growth in the extra-tropics correspond to variability on glacial/interglacial scales. ~~these deviations are climatic in origin because there is less variability in the tropical than the temperate curve. Thus, even at a global level, the speleothem data provide a first-order assessment of climate changes on orbital time scales~~ Thus, the speleothem data indicate similar climatic sensitivity, even at a global level, to that demonstrated for sub-continental and regional scales

by earlier authors, despite their use of much smaller numbers and far less precise age data than in the SISAL dataset.

3.2 How well do the speleothem records represent modern $\delta^{18}O$ in precipitation?

The first-order spatial patterns shown by the SISAL speleothem records during the modern period (1960–2017; n = ~~72~~87) are in overall agreement with the OIPC dataset of interpolated $w\delta^{18}O_p$ (R^2 = 0.~~78~~76), with more negative values at higher latitudes and in more continental climates (Fig. 3a). The fact that the speleothem records reflect the $\delta^{18}O$ patterns in modern precipitation confirms at a global scale the findings of McDermott et al. (2011) for the continental scale in Europe.~~as shown by McDermott et al. (2011) for European stalagmites.~~ There are no systematic biases between OIPC and SISAL data at different latitudes (Fig. 3b). ~~Low latitude sites tend to show more positive $\delta^{18}O$ values than the OIPC data, whereas sites from the mid to high latitudes tend to be more negative (Fig. 3b).~~ However, low latitude sites tend to show more positive $\delta^{18}O$ values than simualted ~~A similar bias is observed in the comparison between SISAL and the simulated~~ $w\delta^{18}O_p$, whereas sites from mid to high latitudes tend to be more negative ~~(R^2 = 0.79), although in this case the slope is steeper~~ (Fig. 3 c, d). The~~Some~~ discrepancies between the SISAL data and the observations or simulations may be due to cave specific factors (such as a preferred seasonality of recharge (e.g., Bar-Matthews et al., 1996), non-equilibrium fractionation processes during speleothem deposition (e.g., Ersek et al., 2018)), ~~or~~ by complex soil-atmosphere interactions affecting evapotranspiration (e.g., Denniston et al., 1999) and~~,~~ thus~~,~~ the isotopic signal of the effective recharge, or uncertainties in the isotope fractionation factors with respect to temperature (Figure S1) amongst others (e.g., Hartmann and Baker, 2017). However, the overall level of agreement suggests that the SISAL data provide a good representation of the impacts of modern hydroclimatic processes.

Comparison of the SISAL records with $\delta^{18}O_p$ weighted according to the potential recharge amount or with $\delta^{18}O_{sw}$ weighted to the moisture amount does not significantly improve the data-model comparison (~~Supplementary~~ Fig. ~~1~~S2). The best relationship is obtained with soil water $\delta^{18}O$ weighted according to soil moisture amount ($w\delta^{18}O_{sw}$~~;~~ (R^2 = 0.~~80~~76). However, smoothing the simulated $w\delta^{18}O_{~~p~~}$ records on a sample-to-sample basis to account for multi-year transit times in the karst environment produces a slightly better geographic agreement with the SISAL records (~~Supplementary~~ Fig. S~~2~~3). Accounting for differences between the model grid cell and cave elevations does not yield any overall improvement in the global correlations.

Simulated inter-annual variability is less than shown in the GNIP data (Fig. 4). Although there are missing values for the GNIP station data, we have also removed these intervals from the simulations,

so incomplete sampling is unlikely to explain the difference between the observed and simulated inter-annual variability. Our results are consistent with the general tendency of climate models to underestimate the sensitivity of extreme precipitation to temperature variability or trends (Flato et al., 2014). ECHAM5 is known to underestimate inter-annual variability in regions where precipitation is dominantly convective (i.e., the tropics), as well as in summer in extra-tropical regions (e.g., in southern Europe) because convective precipitation operates on small spatial scales and has a large random component, even for a given large-scale atmospheric state (Eden et al., 2012). The inter-annual variability of the modern speleothem records is lower than both the simulated and the GNIP data, reflecting the impact of ~~within~~ karst and in-cave processes that effectively act as a low-pass filter on the signal recorded during speleothem growth (Baker et al., 2013). Thus, s~~S~~moothing the simulated $\delta^{18}O_p$ signal produces a better match to the SISAL records: application of a smoothing window of > 6~~5~~ yrs to simulated w$\delta^{18}O_p$ produces a good match (95% confidence) with the inter-annual variability shown by the speleothems (Fig. 4). ~~The fact that the temporal smoothing of the simulations produces a better match both in terms of geographic patterns and inter-annual variability results from the tendency of speleothem records to predominantly contain low-frequency information (Baker et al., 2013) and~~ This result indicates that global data-model comparisons using speleothem records should focus on quasi-decadal or longer timescales. However, the temporal smoothing caused by karst processes varies from site to site; where transmission from the surface to the cave can be shown to be rapid, individual speleothems may preserve annual or even sub-annual signals.

3.3 Anomaly-mode time-slice comparisons

The selection of a modern or pre-industrial base period is a first step in reconstructing speleothem $\delta^{18}O$ anomalies for comparisons with simulated changes in specific model experiments. There are 76~~62~~ speleothem records from 62 sites that cover the pre-industrial interval 1850±15 CE, commonly used as a reference in model experiments. However, using this short interval as the base period for comparisons with MH or LGM simulations would result in the reconstruction of anomalies for only ~~18~~ 21 records for the MH and only ~~5~~ 7 records for the LGM - which are the number of speleothem records with isotopic samples in both the base period and either the MH or LGM (Table 2). There is no significant difference in the mean $\delta^{18}O$ values for this pre-industrial period and the modern $\delta^{18}O$ values (R^2 = 0.96; ~~Supplementary~~ Fig. S~~3~~4). Using an extended modern baseline (1850–1990 CE) increases the data uncertainties by only ±0.5‰ but raises the number of MH records for which MH-modern anomalies can be calculated to 36~~4~~ entities from ~~29~~ 32 sites around the world. There is also an improvement in the number of LGM sites for which it is possible to calculate anomalies, from ~~5~~ 7 to 13~~1~~ entities at 12~~0~~ sites. Although longer base periods have been used for data-model comparisons,

for example the last 1,000 years (e.g., Werner et al., 2016), this would increase the uncertainties in the observations without substantially increasing the number of records for which it would be possible to calculate anomalies, particularly for the LGM (Table 2). We, therefore, recommend the use of the interval 1850–1990 CE as the baseline for calculation of $\delta^{18}O$ anomalies from the speleothem records.

A relatively good agreement exists between the sign of the simulated and observed $\delta^{18}O$ changes at the MH and LGM: ~~77~~94% of the MH entities and ~~64~~84% of the LGM entities show changes in the same direction after allowing for an uncertainty of ±0.5‰ (Fig. 5 a, b). However, the magnitude of the changes is larger in the SISAL records than the simulations. The MH-modern speleothem anomalies range from -3.603 to 1.298‰ (mean±std: -0.508±1.01‰), but the simulated anomalies only range from -0.49~~1.03~~ to 0.~~30~~28‰ (mean±std: ~~-~~0.0013±0.321‰). Observed anomalies are 45~~–~~20 times larger than simulated anomalies in the Asian monsoon region, and in individual sites in North and South America and Uzbekistan (Fig. 5 a). The data-model mismatch is smallest in Europe, with a mean data-model offset of -0.13~~0.24~~±0.420‰ (n = 9 entities from 7 sites). ~~Multivariate analyses (Supplementary Information) also show that there is no significant relationship between observed and simulated $\delta^{18}O$ patterns in the MH.~~ A two-tailed Student t-test shows that most of the simulated ~~anomalies~~ MH values are not significantly different from present (at 95% confidence). This may reflect the fact that the *midHolocene* simulation was only run for 10 years but is also consistent with previous studies which show that climate models substantially underestimate the magnitude of MH changes (Harrison et al., 2014), particularly in monsoon regions (e.g., Perez-Sanz et al., 2014).

The simulated changes in $\delta^{18}O$ at the LGM are much larger than those simulated for the MH and are significant (at 95% confidence) over much of the globe. There is no regionally coherent pattern in the observed LGM anomalies because of the limited number of speleothems that grew continuously from the LGM to present. However, the sign of the observed changes is coherent with the simulated change in $\delta^{18}O$ for 11~~7~~ of the 13~~1~~ records (Fig. 5 b). The magnitude of the LGM anomalies differs by less than 1‰ between model and data in ~~half~~ two thirds of the locations. A strong offset is found in the two records from Sofular Cave, which are ca. 5.5~~6~~‰ more negative than the simulated $\delta^{18}O$. This offset may be related to the glacial changes in the Black Sea region, which are not well represented in the *lgm* simulation. Thus, although overall the comparison with the speleothem records suggests that the simulated changes in hydroclimate are reasonable, the simulated changes in the Middle East differ from observations. ~~However, multivariate analyses (Supplementary Information) reveal no significant relationship between observed and simulated global LGM $\delta^{18}O$ patterns.~~

An alternative approach to examine the realism of simulated changes is to compare the LGM and MH ~~simulations~~ periods directly, which improves the number of records for which anomalies can be

calculated (Fig. 5 c; n = 220). However, the pattern of change is similar to the LGM-modern anomalies. The simulated and observed direction of change is coherent at 860% of the locations with an ~~n~~ offset smaller than 1‰ occurring in ~~7~~ 12 sites and again the largest discrepancy is Sofular Cave. Thus, in this particular example, a direct comparison of the LGM-MH anomalies does not provide additional insight to the comparison of LGM-modern anomalies. Nevertheless, such an approach might be useful for other time periods (e.g., comparison of early versus mid-Holocene) when there are likely to be many more speleothem records available.

Age uncertainties inherent to the speleothem samples ~~selected to~~ representing the LGM could partially explain the LGM data-model mismatches. A global assessment of the impact of time-window width on the MH and LGM anomalies shows that reducing the window width from ±500 to ±200 years in the MH has little impact on the average values (~~Supplementary~~ Fig. S5~~4~~) but reduces the inter-sample variability and produces a better match to the simulated anomalies. A similar analysis for the LGM (~~Supplementary~~ Fig. S6~~5~~) suggests that a window width of ±500 years (rather than ±1,000 years) would be the most appropriate choice for comparisons of this interval. The number of SISAL sites available for such comparisons is not affected. However, analyses of the relative error of the isotope anomalies calculated at individual sites for different LGM window widths (Fig. 6) show a clear increase in all relative error components as window size decreases for BT-2 (Botuverá cave; Fig. 6a; Cruz et al., 2005) but no clear changes in the relative error terms for SSC01 (Gunung-buda cave; Fig. 6b; Partin et al., 2007)~~(the samples from Botuverá and Gunung-buda cave in Figure 6a and 6b, respectively, with new COPRA-produced age-depth models)~~. These results suggest that, with an LGM window width of ±1,000 years, the relative contribution of age uncertainty to the anomaly uncertainty is small (Fig. 6). Thus, although it is clear that it would be useful to propagate age uncertainties for individual sites, changing the conventional definitions of the MH and LGM time slices in deriving speleothem anomalies does not seem warranted at this stage.

3.4 Analysis of spatial gradients

The number of sites available in SISALv1b means that quantitative data-model comparisons using the traditional anomaly approach are limited in scope. Approaches based on comparing trends in absolute $\delta^{18}O$ values could provide a way of increasing the number of observations and an alternative way to evaluate the simulations. Comparison of trends places less weight on anomalous sites and allows large-scale systematic similarities and dissimilarities between model and observations to be revealed. We illustrate this approach using spatial gradients across Asia and across Europe and showing how they differ between the modern, ~~in the~~ MH and LGM periods, although such an approach could also be used for temporal trends.

The first-order ~~trends~~ spatial gradient in observed $\delta^{18}O$ ~~changes~~ during the ~~MH~~ modern period is broadly captured by the model in both examples (Figs. 7, 8), with the largest offsets found mainly for high altitude sites. There is a fundamental change in the latitudinal gradient across Asia during the MH (Fig. 7). In this period, the gradient observed in the data is clearly not reproduced by the model, which systematically simulates higher $w\delta^{18}O_p$ values between 20 and 35°N, suggesting that the model underestimates the insolation-driven intensification of the hydrological cycle in monsoon regions during this period. The limited number of speleothem records available between 25 and 35 °N for the LGM agree with the simulated $\delta^{18}O$ gradient. The longitudinal gradient across Europe (Fig. 8) does not change substantially in the MH compared to modern. However, the model simulates $w\delta^{18}O_p$ values ~2‰ lower than observed in low-altitude sites in south central Europe between 0 and 15°E during the MH. This suggests that model may be underestimating the role of atmospheric circulation (i.e., weaker westerlies) during this period, an aspect of the climate system that models have difficulty to simulate (Mauri et al., 2014). The large latitudinal variability of simulated values eastwards of ~ 5°E during the LGM is consistent with a larger spread in the observations, albeit the limited number of data available. ~~The largest mismatches between the observations and simulations, in the high latitudes of North America, in mid-latitude Europe and in the monsoon region of Asia, are in regions where the model does not reflect the reconstructed MAP. This confirms the suggestion, based on comparison of the MH mapped patterns (section 3.3), that ECHAM5-wiso underestimates changes in precipitation between the MH and the present day. The observed latitudinal $\delta^{18}O$ gradients in the LGM are reasonably well captured by the simulations (Fig. 8), reflecting the strong latitudinal control on $\delta^{18}O$ variability (Dansgaard, 1964). As is the case in the MH, the largest discrepancies occur in regions where the model overestimates MAP. However, this mismatch may partly reflect the fact that the pollen-based reconstructions do not take account of the low atmospheric CO_2 concentration during the glacial and, may consequently underestimate the actual precipitation amount (Prentice et al., 2017).~~ ~~Nevertheless, t~~These examples show the potential to use trends in absolute values for model evaluation and diagnosis.

4 Protocol for data-model comparison using speleothem data

Our analyses illustrate a number of possible approaches for ~~utilising~~ using speleothem isotopic data ~~towards~~ for model evaluation. The discontinuous nature of most speleothem records means that the number of sites available for conventional anomaly-mode comparisons is potentially limited. To some extent this is mitigated by the fact that differences between the modern and pre-industrial isotope values are small, permitting the calculation of anomalies using a longer baseline interval (1850–1990 CE). The use of smaller intervals of time in calculating MH or LGM anomalies (~~Supplementary~~ Fig. S~~4~~ 5

and ~~5~~6) does not have a significant impact either on the mean values or the number of records provided the interval is > ±300 yrs for the MH and > ±500 yrs for the LGM. Although the use of shorter intervals is possible, we recommend using the conventional definitions of each time slice to facilitate comparison with other benchmark datasets. Although patterns in the isotopic anomalies can provide a qualitative assessment of model performance, site-specific factors could lead to large differences from the simulations at individual locations. Improved spatial coverage would allow such sites to be identified and screened out before making quantitative comparisons of observed and simulated anomalies. Although there are only a limited number of records that cover both the modern baseline period and the MH (or the modern baseline period and the LGM), there are many more records that provide information about one or other of these periods. The examination of spatial gradients in absolute $\delta^{18}O$ provides one way of exploiting this larger data coverage~~More records are available for the MH or LGM alone than for both that period (i.e. MH or LGM) and the modern baseline period, encouraging examination of spatial gradients in absolute $\delta^{18}O$~~. Even when an offset between the observed and simulated $\delta^{18}O$ exists, comparing the trends along such gradients is possible. Thus, both absolute values and anomalies of the isotope data for data-model comparison are useful.

Screening of published speleothem isotopic data is essential to produce meaningful data-model comparisons. The SISAL database facilitates screening for mineralogy, which has a substantial effect on isotopic values because of differences in water-carbonate fractionation factors for aragonite or calcite that are more pronounced at lower temperatures (Fig. S1). We recommend the use of the empirical speleothem-based fractionation factor of Tremaine et al. (2011) for isotope values on calcite stalagmites, or on aragonite specimens that have been corrected to their calcite equivalent in the original publications, and the equilibrium fractionation equation of Grossman and Ku (1986) for aragonite samples to ensure consistency across records.

Based on the limited number of records available at the LGM, speleothem age uncertainties have only a limited impact on mean isotopic values, propagation of such uncertainties as well as any model uncertainties would nevertheless substantially improve the robustness of data-model comparisons.

Based on our analyses, we therefore recommend that model evaluation using speleothem records should:

1. Filter speleothem records with respect to their mineralogy and use the appropriate equilibrium fractionation factor: Tremaine et al. (2011) for converting isotopic data from either calcite or aragonite-corrected-to-calcite samples to their drip water equivalent; and Grossman and Ku (1986) as reformulated by Lachniet (2015) for converting isotopic data from aragonite samples;

2. U~~u~~se the interval between 1850 and 1990 as the reference period for speleothem isotope records;
3. ~~use~~ Use speleothem isotopic data averaged for the intervals 6,000 ±500 yrs (21,000 ±1,000 yrs) for comparability with other MH (LGM) palaeoclimate benchmark datasets;
4. ~~use~~ Use speleothem isotopic data averaged for the interval 6,000 ±200 yrs or 21,000 ±500 yrs for best approximation of *midHolocene* and *lgm* experiments;
5. ~~use~~ Use absolute values only to assess data-model first order spatial patterns;
6. ~~focus~~ Focus on multi-decadal to millennial timescales if using transient simulations for data-model comparisons.

5 Conclusions

Speleothem records show the same first-order spatial patterns as available in the Global Network of Isotopes in Precipitation (GNIP) data~~,~~ and~~, therefore,~~ are therefore a good reflection of the $\delta^{18}O$ patterns in modern precipitation. This observation ~~then~~ suggests that stalagmites are a rich source of information for model evaluation. However, the inter-annual variability in the modern speleothem records is considerably reduced compared to the simulations, which in turn show less inter-annual variability than the GNIP observations. The low variability shown by the SISAL records – most likely from the low-pass filter effectively applied to the speleothem record by the karst system – precludes the use of this database for global studies focused on time scales shorter than quasi-decadal ~~on a global basis~~.

Using the traditional anomaly approach to data-model comparisons, there is consistency between the sign of observed and simulated changes in both the MH and the LGM ~~exists~~. However, the ECHAM5-wiso model underestimates the changes in $\delta^{18}O$ between time periods compared to the speleothems records (i.e., the amplitude of modelled $\delta^{18}O$ changes is lower). ~~than the amplitude observed in the speleothem records.~~ Thus, these kinds of comparisons should only focus on the large-scale spatial patterns ~~that are significant, robust and climatologically interpretable~~. Based on the available SISAL data, the use of smaller time windows than the conventional definitions for each time slice does not have a strong impact on the mean values and could be used to reduce the uncertainties associated with the palaeodata. However, this would preclude comparisons with existing benchmark datasets that use the conventional windows for the MH and LGM time slices.

Only a limited number of speleothem records are continuous over long periods of time and the need to convert these to anomalies with respect to modern is a drawback. The limited number of records covering the LGM make the comparisons for this period particularly challenging. Nevertheless,

continued expansion of SISAL database will increase its usefulness for model evaluation in future. Furthermore, we have shown that alternative approaches using absolute values could help examine spatial trends and diagnose systematic offsets.

~~Difficulties in constraining structural error on the model side and local controls on the observations complicate the derivation of comprehensive estimates of the true uncertainties of both simulations and observations. Site-specific controls can affect the $\delta^{18}O$ record captured in speleothems, but we have not screened for regionally anomalous records that could be influencing the results in our analyses. Our initial analyses suggest age uncertainty contributes little to the estimates for the LGM speleothem isotopic values. However, it is still important to propagate dating uncertainties for data-model comparison. Despite these challenges, SISAL appears to be an extremely useful tool for describing past patterns of variability, highlighting its potential for evaluating CMIP6-PMIP4 experiments.~~ Mismatches between simulations and observations can reflect the issues with the experimental design, problems with the model or uncertainties in the observations (Harrison et al., 2015). The failure to include changes in atmospheric dust loading, for example, has been put forward as an explanation of data-model mismatches in both the MH and the LGM (e.g., Hopcroft et al., 2015; Messori et al., 2019). Missing processes and feedbacks, such as climate-induced vegetation or land-surface changes, could also contribute to mismatches (e.g., Yoshimori et al., 2009; Swann et al., 2014). Uncertainties caused by the specific structure of the model or assigned model parameter values could also contribute to data-model mismatches (Qian et al., 2016). Ultimately, there needs to be an assessment of the contribution of all of these factors to data-model mismatches, but here we have only focused on potential uncertainties associated with the speleothem data. Our initial analyses suggest age uncertainty contributes little to the uncertainties in the estimates of LGM speleothem isotopic values. However, it is still important to propagate dating uncertainties for data-model comparison. Site-specific controls may have a much larger effect on the $\delta^{18}O$ record recorded by individual speleothems and thus may contribute significantly to uncertainties in local or regional signals. We have not screened for regionally anomalous records that could be influencing the results of our analyses, but this should certainly be done. Despite these challenges, SISAL appears to be an extremely useful tool for describing past patterns of variability, highlighting its potential for evaluating CMIP6-PMIP4 experiments.

Comparisons with speleothem data can be seen as a complement to model evaluation using other types of palaeoenvironmental data and palaeoclimatic reconstructions (see e.g., MARGO project members, 2009; Harrison et al., 2014). They are particularly useful because they provide insights into how well state-of-the-art models reproduce the hydrological cycle and atmospheric circulation

patterns. The ability to reproduce past observations provides additional confidence in the ability of climate models to simulate large climate changes, such as those expected by the end of the 21st century (Braconnot et al., 2012; Schmidt et al., 2014). However, mismatches between model simulations and palaeo-observations are also useful because they can help to pinpoint issues that may need to be addressed in developing improved models or in better experimental protocols (Kageyama et al., 2018), providing that these mismatches do not arise because of misunderstanding or misinterpretation of the observations themselves. By providing a protocol for using speleothem data for data-model comparisons that accounts for uncertainties in the observations, we anticipate that at least such causes of data-model mismatches will be minimized.

6 Data availability

~~The version of the SISAL database used in this study is available in the University of Reading Research Data Archive (http://dx.doi.org/10.17864/1947.189). This dataset is cited in this manuscript as Atsawawaranunt et al., 2019.~~The SISAL (Speleothem Isotopes Synthesis and AnaLysis Working Group) database version 1b is publicly available through the University of Reading repository at http://doi.org/10.17864/1947.189 (Atsawawaranunt et al., 2019) and through the NOAA's National Centers for Environmental Information (NCEI) at https://www.ncdc.noaa.gov/paleo-search/study/24070. The ECHAM5-wiso model output is available from https://doi.org/10.1594/PANGAEA.902347 (Werner, 2019). The OIPC mean annual precipitation $\delta^{18}O$ data is available from the Water Isotopes Database at http://wateriso.utah.edu/waterisotopes/pages/data_access/ArcGrids.html (Bowen and Revenaugh, 2003; IAEA/WMO, 2015; Bowen, 2018). The Global Network of Isotopes in Precipitation (GNIP) data from the International Atomic Energy Agency (IAEA) and the World Meteorological Organization (WMO) is available at https://nucleus.iaea.org/wiser upon registration (IAEA/WMO, 2018).

7 Team list

SISAL working group members who coordinated data gathering for the SISAL database (listed in alphabetical order): Syed Masood Ahmad (Department of Geography, Faculty of Natural Sciences, Jamia Millia Islamia, New Delhi 110025, India), Yassine Ait Brahim (Institute of Global Environmental Change, Xi'an Jiaotong University, Xi'an, Shaanxi, China), Sahar Amirnezhad Mozhdehi (School of Earth Sciences, University College Dublin, Belfield. Dublin 4, Ireland), Monica Arienzo (Division of Hydrologic Sciences, Desert Research Institute, 2215 Raggio Parkway, 89512 Reno, NV, USA), Kamolphat Atsawawaranunt (School of Archaeology, Geography & Environmental Sciences, Reading University, Whiteknights, Reading, RG6 6AH, UK), Andy Baker (School of Biological, Earth and Environmental

Sciences, University of New South Wales, Kensington 2052, Australia), Kerstin Braun (Institute of Human Origins, Arizona State University, PO Box 874101, 85287 Tempe, Arizona, USA), Sebastian Breitenbach (Sediment & Isotope Geology, Institute of Geology, Mineralogy & Geophysics, Ruhr-Universität Bochum, Universitätsstr. 150, IA E5-179, 44801 Bochum, Germany), Yuval Burstyn (Geological Survey of Israel, 32 Yesha'yahu Leibowitz, 9371234, Jerusalem, Israel; Institute of Earth Sciences, Hebrew University of Jerusalem, Edmond J. Safra campus, Givat Ram, 91904 Jerusalem, Israel), Sakonvan Chawchai (MESA Research unit, Department of Geology, Faculty of Sciences, Chulalongkorn University, 254 Phayathai Rd, Pathum Wan, 10330 Bangkok, Thailand), Andrea Columbu (Department of Biological, Geological and Environmental Sciences, Via Zamboni 67, 40126, Bologna, Italy), Michael Deininger (Institute of Geosciences, Johannes Gutenberg University Mainz, Johann-Joachim-Becher-Weg 21, 55128 Mainz, Germany), Attila Demény (Institute for Geological and Geochemical Research, Research Centre for Astronomy and Earth Sciences, Hungarian Academy of Sciences, Budaörsi út 45, H-1112 Budapest, Hungary), Bronwyn Dixon (School of Archaeology, Geography & Environmental Sciences, Reading University, Whiteknights, Reading, RG6 6AH, UK and School of Geography, University of Melbourne, Melbourne, 3010, Australia), István Gábor Hatvani (Institute for Geological and Geochemical Research, Research Centre for Astronomy and Earth Sciences, Hungar~~y~~ian), Jun Hu (Department of Earth Sciences, University of Southern California, 3651 Trousdale Parkway, 90089 Los Angeles, California, USA), Nikita Kaushal (Department of Earth Sciences, University of Oxford, South Parks Road, Oxford, OX1 3AN, UK), Zoltán Kern (Institute for Geological and Geochemical Research, Research Centre for Astronomy and Earth Sciences, Hungarian Academy of Sciences, Budaörsi út 45, H-1112 Budapest, Hungary), Inga Labuhn (Institute of Geography, University of Bremen, Celsiusstr. 2, 28359 Bremen, Germany), Matthew S. Lachniet (Dept. of Geoscience, University of Nevada Las Vegas, Box 4022, 89154 Las Vegas, NV, USA), Franziska A. Lechleitner (Department of Earth Sciences, University of Oxford, South Parks Road, OX1 3AN Oxford, UK), Andrew Lorrey (National Institute of Water & Atmospheric Research, Climate Atmosphere and Hazards Centre, 41 Market Place, Viaduct Precinct, Auckland, New Zealand), Monika Markowska (University of Tübingen, Hölderlinstr. 12, 72074 Tübingen, Germany), Carole Nehme (IDEES UMR 6266 CNRS, Geography department, University of Rouen Normandie, Mont Saint Aignan, France), Valdir F. Novello (Instituto de Geociências, Universidade de São Paulo, São Paulo, Brazil), Jessica Oster (Department of Earth and Environmental Sciences, Vanderbilt University, Nashville, TN, 37206, USA), Carlos Pérez-Mejías (Department of Geoenvironmental Processes and Global Change, Pyrenean Institute of Ecology (IPE-CSIC), Avda. Montañana 1005, 50059 Zaragoza, Spain), Robyn Pickering (Department of Geological Sciences, University of Cape Town, University Avenue, Upper Campus, Room 208, 7701 Rondebosch, Cape Town, South Africa), Natasha Sekhon (Department of Geological

Sciences, Jackson School of Geosciences, University of Texas, Austin, TX, 78712, USA), Xianfeng Wang (Earth Observatory of Singapore, Nanyang Technological University, Singapore 636798), Sophie Warken (Institute of Environmental Physics, Ruprecht-Karls-Universität Heidelberg, Im Neuenheimer Feld 229, 69120 Heidelberg, Germany.

SISAL working members who submitted data to the SISAL database (listed in alphabetical order): Tim Atkinson (Departments of Earth Sciences & Geography, University College London, WC1E 6BT, United Kingdom), Avner Ayalon (Geological Survey of Israel, 32 Yesha'yahu Leibowitz, Jerusalem, 9371234), James Baldini (Department of Earth Sciences, Durham University, DH1 3LE, United Kingdom), Miryam Bar-Matthews (Geological Survey of Israel, 32 Yesha'yahu Leibowitz, Jerusalem, 9371234), Juan Pablo Bernal (Centro de Geociencias, Universidad Nacional Autónoma de México, Campus UNAM Juriquilla, Querétaro 76230, Querétaro, Mexico), Ronny Boch (Graz University of Technology. Institute of Applied Geosciences. Rechbauerstrasse 12, 8010 Graz, Austria), Andrea Borsato (School of Environmental and Life Science, University of Newcastle, 2308 NSW, Australia), Meighan Boyd (Department of Earth Sciences, Royal Holloway University of London, Egham, Surrey TW20 0EX, UK), Chris Brierley (Department of Geography, University College London, WC1E 6BT, United Kingdom), Yanjun Cai (State Key Lab of Loess and Quaternary Geology, Institute of Earth Environment, Chinese Academy of Sciences, Xi'an 710061, China), Stacy Carolin (Institute of Geology, University of Innsbruck, Innrain 52, 6020 Innsbruck, Austria), Hai Cheng (Institute of Global Environmental Change, Xi'an Jiaotong University, China), Silviu Constantin (Emil Racovita Institute of Speleology, str. Frumoasa 31, Bucharest, Romania), Isabelle Couchoud (EDYTEM, UMR 5204 CNRS, Université Savoie Mont Blanc, Université Grenoble Alpes, 73370 Le Bourget du Lac, France), Francisco Cruz (Instituto de Geociências, Universidade de São Paulo, São Paulo, Brazil), Rhawn Denniston (Department of Geology, Cornell College, Mount Vernon, IA, 52314, USA), Virgil Drăguşin (Emil Racovita Institute of Speleology, str. Frumoasa 31, Bucharest, Romania), Wuhui Duan (Key Laboratory of Cenozoic Geology and Environment, Institute of Geology and Geophysics, Chinese Academy of Sciences, Beijing, China, 100029, Vasile Ersek (Department of Geography and Environmental Sciences, Northumbria University, Newcastle upon Tyne, UK), Martin Finné (Department of Archaeology and Ancient History, Uppsala University, Sweden), Dominik Fleitmann (Department of Archaeology. School of Archaeology, Geography and Environmental Science. Whiteknights. University of Reading RG6 6AB, UK), Jens Fohlmeister (Institute for Earth and Environmental Sciences, University of Potsdam, Karl-Liebknecht-Str. 24-25, 14476 Potsdam, Germany), Amy Frappier (Department of Geosciences, Skidmore College, Saratoga Springs, NY 12866 US), Dominique Genty (Laboratoire des Science du Climat et de l'Environment, CNRS, L'Orme des Merisiers, 91191 Gif-sure-Yvette Cedex, France), Steffen Holzkämper (Department of Physical Geography. Stockholm University. 106 91 Stockholm, Sweden),

Philip Hopley (Department of Earth and Planetary Sciences, Birkbeck, University of London, Malet St, London, WC1E 7HX), Vanessa Johnston (Karst Research Institute, Research Centre of the Slovenian Academy of Sciences and Arts, Titov trg 2, SI-6230, Postojna, Slovenia), Gayatri Kathayat (Institute of Global Environmental Change, Xi'an Jiaotong University, China), Duncan Keenan-Jones (School of Historical and Philosophical Inquiry, University of Queensland, St Lucia QLD 4072, Australia), Gabriella Koltai (Institute of Geology, University of Innsbruck, Innrain 52, 6020 Innsbruck, Austria), Ting-Yong Li (Chongqing Key Laboratory of Karst Environment, School of Geographical Sciences, Southwest University, Chongqing 400715, China, and Field Scientific Observation & Research Base of Karst Eco-environments at Nanchuan in Chongqing, Ministry of Nature Resources of China, Chongqing 408435, China), Marc Luetscher (Swiss Institute for Speleology and Karst Studies (SISKA), Rue de la Serre 68, CH-2301 La Chaux-de-Fonds, Switzerland), Dave Mattey (Department of Earth Sciences, Royal Holloway University of London, Egham, Surrey, TW20 0EX, UK), Ana Moreno (Dpto. de Procesos Geoambientales y Cambio Global. Instituto Pirenaico de Ecología-CSIC. Zaragoza, Spain), Gina Moseley (Institute of Geology, University of Innsbruck, Innrain 52, 6020 Innsbruck, Austria), David Psomiadis (Imprint Analytics GmbH, Werner von Siemens Str. 1, A7343 Neutal, Austria), Jiaoyang Ruan (Guangdong Provincial Key Lab of Geodynamics and Geohazards, School of Earth Sciences and Engineering, Sun Yat-sen University, Guangzhou 510275, China), Denis Scholz (Institute for Geosciences, University of Mainz, Johann-Joachim-Becher-Weg 21, 55128 Mainz, Germany), Lijuan Sha (Institute of Global Environmental Change, Xi'an Jiaotong University, Xi'an, Shaanxi, China), James Baucher 5, Sofia 1164, Bulgaria), Andrew Christopher Smith (NERC Isotope Geoscience Facility, British Geological Survey, Nottingham, UK), Nicolás Strikis (Departamento de Geoquímica, Universidade Federal Fluminense, Niterói, Brazil), Pauline Treble (ANSTO, Lucas Heights NSW, Australia), Ezgi Ünal-İmer (Department of Geological Engineering, Middle East Technical University, Ankara, Turkey), Anton Vaks (Geological Survey of Israel, 32 Yesha'yahu Leibowitz, Jerusalem, 9371234), Stef Vansteenberge (Analytical, Environmental & Geo-Chemistry, Department of Chemistry, Vrije Universiteit Brussel, Belgium), Ny Riavo G. Voarintsoa (Institute of Earth Sciences, The Hebrew University in Jerusalem, Israel), Corinne Wong (Environmental Science Institute, The University of Texas at Austin, 2275 Speedway, Austin TX 78712, USA), Barbara Wortham (Department of Earth and Planetary Science, University of California, Davis, USA), Jennifer Wurtzel (Research School of Earth Sciences, Australian National University, Canberra, ACT, Australia / ARC Centre of Excellence for Climate System Science, Australian National University, Canberra, ACT, Australia), Haiwei Zhang (Institute of Global Environmental Change, Xi'an Jiaotong University, China).

14 Author contribution

LCB is the coordinator of the SISAL working group. LCB and SPH designed the study. LCB and SPH wrote the first draft of the manuscript with contributions from MW, NS, KR, CVP. LCB did the analyses and created Figs. 1, 32-5, 7, 8 and Supplementary Figs., S1-65. MW provided the ECHAM5-wiso model simulations and helped on itswith model analyses. NS did the analyses on speleothem growth over time and created Fig. 2. KR did the analysis on the LGM uncertainties and created Fig. 6. CVP did the multivariate linear analyses (Supplementary material). All authors contributed to the last version of this manuscript. The authors listed in the "SISAL working group" team contributed to this study coordinating data gathering, database construction or with speleothem data submitted to the SISAL database. SB created the COPRA age-depth models used in this study. TA and DG contributed original unpublished data to the SISAL database. AB, BW, JB, AB, ZK, MA, MSL, SB, TA, VJ, BW and SBZK helped edit the manuscript.

15 Competing interests

The authors declare that they have no conflict of interest.

16 Acknowledgements

SISAL (Speleothem Isotopes Synthesis and Analysis) is a working group of the Past Global Changes (PAGES) programme. We thank PAGES for their support for this activity. Additional financial support for SISAL activities has been provided by the European Geosciences Union (EGU TE Winter call, grant number W2017/413), Irish Centre for Research in Applied Geosciences (iCRAG), European Association of Geochemistry (Early Career Ambassadors program 2017), Quaternary Research Association UK, Navarino Environmental Observatory, Stockholm University, Savillex, John Cantle, University of Reading (UK), University College Dublin (Ireland; Seed Funding award, grant number SF1428), and University Ibn Zohr (Morocco). LCB and SPH acknowledge support from the ERC-funded project GC2.0 (Global Change 2.0: Unlocking the past for a clearer future, grant number 694481). SPH also acknowledges support from the JPI-Belmont project "PAleao-Constraints on Monsoon Evolution and Dynamics (PACMEDY)" through the UK Natural Environmental Research Council (NERC). LCB also acknowledges support from the Geological Survey Ireland (Short Call 2017; grant number 2017-SC-056) and the Royal Irish Academy's Charlemont Scholar award 2018. CVP acknowledges funding from the Portuguese Science Foundation (FCT) through the CIMA research center project (UID/MAR/00350/2013). KR was supported by Deutsche Forschungsgemeinschaft (DFG) grant no. RE3994/2-1. We thank the World Karst Aquifer Mapping project (WOKAM) team for providing us with the karst map presented in Fig. 1a. The authors would like to thank the following data contributors: Petra Bajo, Dominique Blamart, Russell Drysdale, Frank McDermott and Jean Riotte.

17 References

Atkinson, T. C., Harmon, R. S., Smart, P. L., and Waltham, A. C.: Palaeoclimatic and geomorphic implications of 230Th/234U dates on speleothems from Britain, Nature, 272, 24-28, https://doi.org/10.1038/272024a0, 1978.

Atsawawaranunt, K., Comas-Bru, L., Amirnezhad Mozhdehi, S., Deininger, M., Harrison, S. P., Baker, A., Boyd, M., Kaushal, N., Ahmad, S. M., Ait Brahim, Y., Arienzo, M., Bajo, P., Braun, K., Burstyn, Y., Chawchai, S., Duan, W., Hatvani, I. G., Hu, J., Kern, Z., Labuhn, I., Lachniet, M., Lechleitner, F. A., Lorrey, A., Pérez-Mejías, C., Pickering, R., Scroxton, N., and Members, S. W. G.: The SISAL database: a global resource to document oxygen and carbon isotope records from speleothems, Earth Syst. Sci. Data, 10, 1687-1713, https://doi.org/10.5194/essd-10-1687-2018, 2018a.

Atsawawaranunt, K., Harrison, S. and Comas-Bru, L.: SISAL (Speleothem Isotopes Synthesis and AnaLysis Working Group) database Version 1.0. University of Reading. Dataset https://doi.org/10.17864/1947.147 2018b.

Atsawawaranunt, K., Harrison, S. and Comas-Bru, L.: SISAL (Speleothem Isotopes Synthesis and AnaLysis Working Group) database Version 1b. University of Reading. Dataset https://doi.org/10.17864/1947.189, 2019.

Ayliffe, L. K., Marianelli, P. C., Moriarty, K. C., Wells, R. T., McCulloch, M. T., Mortimer, G. E., and Hellstrom, J. C.: 500 ka precipitation record from southeastern Australia: Evidence for interglacial relative aridity, Geology, 26, 147-150, https://doi.org/10.1130/0091-7613(1998)026<0147:kprfsa>2.3.co;2, 1998.

Badertscher, S., Fleitmann, D., Cheng, H., Edwards, R. L., Göktürk, O. M., Zumbühl, A., Leuenberger, M., and Tüysüz, O.: Pleistocene water intrusions from the Mediterranean and Caspian seas into the Black Sea, Nature Geoscience, 4, 236-239, 10.1038/ngeo1106, 2011.

Baker, A., Smart, P. L., and Ford, D. C.: NORTHWEST EUROPEAN PALEOCLIMATE AS INDICATED BY GROWTH FREQUENCY VARIATIONS OF SECONDARY CALCITE DEPOSITS, Palaeogeography Palaeoclimatology Palaeoecology, 100, 291-301, 10.1016/0031-0182(93)90059-r, 1993.

Baker, A., Bradley, C., and Phipps, S. J.: Hydrological modeling of stalagmite δ18O response to glacial-interglacial transitions, Geophysical Research Letters, 40, 3207-3212, https://doi.org/10.1002/grl.50555, 2013.

Bar-Matthews, M., Ayalon, A., Matthews, A., Sass, E., and Halicz, L.: Carbon and oxygen isotope study of the active water-carbonate system in a karstic Mediterranean cave: Implications for

paleoclimate research in semiarid regions, Geochimica et Cosmochimica Acta, 60, 337-347, https://doi.org/10.1016/0016-7037(95)00395-9, 1996.

Bar-Matthews, M., Ayalon, A., Gilmour, M., Matthews, A., and Hawkesworth, C. J.: Sea–land oxygen isotopic relationships from planktonic foraminifera and speleothems in the Eastern Mediterranean region and their implication for paleorainfall during interglacial intervals, Geochimica et Cosmochimica Acta, 67, 3181-3199, 10.1016/S0016-7037(02)01031-1, 2003.

Bartlein, P. J., Harrison, S. P., Brewer, S., Connor, S., Davis, B. A. S., Gajewski, K., Guiot, J., Harrison-Prentice, T. I., Henderson, A., Peyron, O., Prentice, I. C., Scholze, M., Seppä, H., Shuman, B., Sugita, S., Thompson, R. S., Viau, A. E., Williams, J., and Wu, H.: Pollen-based continental climate reconstructions at 6 and 21 ka: a global synthesis, Climate Dynamics, 37, 775-802, https://doi.org/10.1007/s00382-010-0904-1, 2011.

Boch, R., Cheng, H., Spötl, C., Edwards, R. L., Wang, X., and Häuselmann, P.: NALPS: a precisely dated European climate record 120–60 ka, Climate of the Past, 7, 1247-1259, 10.5194/cp-7-1247-2011, 2011.

Bowen, G. J., and Revenaugh, J.: Interpolating the isotopic composition of modern meteoric precipitation, Water Resources Research, 39, https://doi.org/10.1029/2003WR002086, 2003.

Braconnot, P., Harrison, S. P., Kageyama, M., Bartlein, P. J., Masson-Delmotte, V., Abe-Ouchi, A., Otto-Bliesner, B., and Zhao, Y.: Evaluation of climate models using palaeoclimatic data, Nature Climate Change, 2, 417, https://doi.org/10.1038/nclimate1456, 2012.

Breitenbach, S. F. M., Rehfeld, K., Goswami, B., Baldini, J. U. L., Ridley, H. E., Kennett, D. J., Prufer, K. M., Aquino, V. V., Asmerom, Y., Polyak, V. J., Cheng, H., Kurths, J., and Marwan, N.: COnstructing Proxy Records from Age models (COPRA), Clim. Past, 8, 1765-1779, https://doi.org/10.5194/cp-8-1765-2012, 2012.

Breitenbach, S. F. M., Lechleitner, F. A., Meyer, H., Diengdoh, G., Mattey, D., and Marwan, N.: Cave ventilation and rainfall signals in dripwater in a monsoonal setting – a monitoring study from NE India, Chemical Geology, 402, 111-124, https://doi.org/10.1016/J.CHEMGEO.2015.03.011, 2015.

Bustamante, M. G., Cruz, F. W., Vuille, M., Apaéstegui, J., Strikis, N., Panizo, G., Novello, F. V., Deininger, M., Sifeddine, A., Cheng, H., Moquet, J. S., Guyot, J. L., Santos, R. V., Segura, H., and Edwards, R. L.: Holocene changes in monsoon precipitation in the Andes of NE Peru based on δ18O speleothem records, Quaternary Science Reviews, 146, 274-287, 10.1016/J.QUASCIREV.2016.05.023, 2016.

Butzin, M., Werner, M., Masson-Delmotte, V., Risi, C., Frankenberg, C., Gribanov, K., Jouzel, J., and Zakharov, V. I.: Variations of oxygen-18 in West Siberian precipitation during the last 50 years, Atmos. Chem. Phys., 14, 5853-5869, https://doi.org/10.5194/acp-14-5853-2014, 2014.

Caley, T., and Roche, D. M.: delta O-18 water isotope in the iLOVECLIM model (version 1.0) - Part 3: A palaeo-perspective based on present-day data-model comparison for oxygen stable isotopes in carbonates, Geoscientific Model Development, 6, 1505-1516, https://doi.org/10.5194/gmd-6-1505-2013, 2013.

Caley, T., Roche, D. M., Waelbroeck, C., and Michel, E.: Oxygen stable isotopes during the Last Glacial Maximum climate: perspectives from data-model (iLOVECLIM) comparison, Climate of the Past, 10, 1939-1955, https://doi.org/10.5194/cp-10-1939-2014, 2014.

Chen, Z., Auler, A. S., Bakalowicz, M., Drew, D., Griger, F., Hartmann, J., Jiang, G., Moosdorf, N., Richts, A., Stevanovic, Z., Veni, G., and Goldscheider, N.: The World Karst Aquifer Mapping project: concept, mapping procedure and map of Europe, Hydrogeology Journal, 25, 771-785, https://doi.org/10.1007/s10040-016-1519-3, 2017.

Cheng, H., Fleitmann, D., Edwards, R. L., Wang, X., Cruz, F. W., Auler, A. S., Mangini, A., Wang, Y., Kong, X., Burns, S. J., and Matter, A.: Timing and structure of the 8.2 kyr B.P. event inferred from δ18O records of stalagmites from China, Oman, and Brazil, Geology, 37, 1007-1010, https://doi.org/10.1130/G30126A.1, 2009.

Cheng, H., Sinha, A., Cruz, F. W., Wang, X., Edwards, R. L., d'Horta, F. M., Ribas, C. C., Vuille, M., Stott, L. D., and Auler, A. S.: Climate change patterns in Amazonia and biodiversity, Nature Communications, 4, 1411-1411, https://doi.org/10.1038/ncomms2415, 2013.

Christensen, J. H., Kanikicharla, K. K., Marshall, G., and Turner, J.: Climate phenomena and their relevance for future regional climate change, in: Climate Change 2013 – The Physical Science Basis: Working Group I Contribution to the Fifth Assessment Report of the Intergovernmental Panel on Climate Change, edited by: Change, I. P. o. C., Cambridge University Press, Cambridge, 1217-1308, 2013.

Collins, M., Knutti, R., Arblaster, J., Dufresne, J.-L., Fichefet, T., Friedlingstein, P., Gao, X., Gutowski, W., Johns, T., and Krinner, G.: Long-term climate change: projections, commitments and irreversibility, in: Climate Change 2013 – The Physical Science Basis: Working Group I Contribution to the Fifth Assessment Report of the Intergovernmental Panel on Climate Change, edited by: Change, I. P. o. C., Cambridge University Press, Cambridge, 1029-1136, 2013.

Collins, W. D., Bitz, C. M., Blackmon, M. L., Bonan, G. B., Bretherton, C. S., Carton, J. A., Chang, P., Doney, S. C., Hack, J. J., Henderson, T. B., Kiehl, J. T., Large, W. G., McKenna, D. S., Santer, B. D., and Smith, R. D.: The Community Climate System Model Version 3 (CCSM3), Journal of Climate, 19, 2122-2143, https://doi.org/10.1175/jcli3761.1, 2006.

Columbu, A., Sauro, F., Lundberg, J., Drysdale, R., and De Waele, J.: Palaeoenvironmental changes recorded by speleothems of the southern Alps (Piani Eterni, Belluno, Italy) during four interglacial to glacial climate transitions, Quaternary Science Reviews, 197, 319-335, https://doi.org/10.1016/J.QUASCIREV.2018.08.006, 2018.

Comas-Bru, L., and Harrison, S. P.: SISAL: Bringing added value to speleothem research, Quaternary, 2(1), https://doi.org/10.3390/quat2010007, 2019.

Coplen, T. B., Kendall, C., and Hopple, J.: Comparison of stable isotope reference samples, Nature, 302, 236-238, https://doi.org/10.1038/302236a0, 1983.

Cosford, J., Qing, H., Eglington, B., Mattey, D., Yuan, D., Zhang, M., and Cheng, H.: East Asian monsoon variability since the Mid-Holocene recorded in a high-resolution, absolute-dated aragonite speleothem from eastern China, Earth and Planetary Science Letters, 275, 296-307, https://doi.org/10.1016/J.EPSL.2008.08.018, 2008a.

Cosford, J., Qing, H., Yuan, D., Zhang, M., Holmden, C., Patterson, W., and Hai, C.: Millennial-scale variability in the Asian monsoon: Evidence from oxygen isotope records from stalagmites in southeastern China, Palaeogeography, Palaeoclimatology, Palaeoecology, 266, 3-12, 10.1016/J.PALAEO.2008.03.029, 2008b.

Cruz, F. W., Burns, S. J., Karmann, I., Sharp, W. D., Vuille, M., Cardoso, A. O., Ferrari, J. A., Dias, P. L. S., and Viana, O.: Insolation-driven changes in atmospheric circulation over the past 116,000 years in subtropical Brazil, Nature, 434, 63-66, https://doi.org/10.1038/nature03365, 2005.

Daëron, M., Drysdale, R. N., Peral, M., Huyghe, D., Blamart, D., Coplen, T. B., Lartaud, F., and Zanchetta, G.: Most Earth-surface calcites precipitate out of isotopic equilibrium, Nature Communications, 10, 429, https://doi.org/10.1038/s41467-019-08336-5, 2019.

Denniston, R. F., González, L. A., Asmerom, Y., Baker, R. G., Reagan, M. K., and Bettis, E. A.: Evidence for increased cool season moisture during the middle Holocene, Geology, 27, 815-815, https://doi.org/10.1130/0091-7613(1999)027<0815:EFICSM>2.3.CO;2, 1999.

Denniston, R. F., Asmerom, Y., Polyak, V., Dorale, J. A., Carpenter, S. J., Trodick, C., Hoye, B., and González, L. A.: Synchronous millennial-scale climatic changes in the Great Basin and the North Atlantic during the last interglacial, Geology, 35, 619-619, 10.1130/G23445A.1, 2007a.

Denniston, R. F., DuPree, M., Dorale, J. A., Asmerom, Y., Polyak, V. J., and Carpenter, S. J.: Episodes of late Holocene aridity recorded by stalagmites from Devil's icebox Cave, Central Missouri, USA, Quaternary Research, 68, 45-52, https://doi.org/10.1016/j.yqres.2007.04.001, 2007b.

Denniston, R. F., Wyrwoll, K.-H., Polyak, V. J., Brown, J. R., Asmerom, Y., Wanamaker, A. D., LaPointe, Z., Ellerbroek, R., Barthelmes, M., Cleary, D., Cugley, J., Woods, D., and Humphreys, W. F.: A Stalagmite record of Holocene Indonesian–Australian summer monsoon variability from the Australian tropics, Quaternary Science Reviews, 78, 155-168, 10.1016/J.QUASCIREV.2013.08.004, 2013.

Dykoski, C. A., Edwards, R. L., Cheng, H., Yuan, D., Cai, Y., Zhang, M., Lin, Y., Qing, J., An, Z., and Revenaugh, J.: A high-resolution, absolute-dated Holocene and deglacial Asian monsoon record from Dongge Cave, China, Earth and Planetary Science Letters, 233, 71-86, https://doi.org/10.1016/J.EPSL.2005.01.036, 2005.

Eden, J. M., Widmann, M., Grawe, D., and Rast, S.: Skill, correction, and downscaling of GCM-simulated precipitation, Journal of Climate, 25, 3970-3984, 2012.

Ersek, V., Onac, B. P., and Persoiu, A.: Kinetic processes and stable isotopes in cave dripwaters as indicators of winter severity, Hydrological Processes, 32, 2856-2862, 10.1002/hyp.13231, 2018.

Fairchild, I., and Baker, A.: Speleothem Science: From Process to Past Environments, Blackwell Quaternary Geoscience Series, edited by: Bradley, R., Wiley-Blackwell, United Kingdom, 432 pp., 2012.

Fensterer, C., Scholz, D., Hoffmann, D., Mangini, A., and Pajón, J. M.: ²³⁰ Th/U-dating of a late Holocene low uranium speleothem from Cuba, IOP Conference Series: Earth and Environmental Science, 9, 012015-012015, https://doi.org/10.1088/1755-1315/9/1/012015, 2010.

Fensterer, C., Scholz, D., Hoffmann, D., Spötl, C., Pajón, J. M., and Mangini, A.: Cuban stalagmite suggests relationship between Caribbean precipitation and the Atlantic Multidecadal Oscillation during the past 1.3 ka, The Holocene, 22, 1405-1412, 10.1177/0959683612449759, 2012.

Field, C. B.: Climate change 2014–Impacts, adaptation and vulnerability: Regional aspects, Cambridge University Press, 2014.

Fischer, M. J., and Treble, P. C.: Calibrating climate-delta O-18 regression models for the interpretation of high-resolution speleothem delta O-18 time series, Journal of Geophysical Research-Atmospheres, 113, https://doi.org/10.1029/2007jd009694, 2008.

Flato, G., Marotzke, J., Abiodun, B., Braconnot, P., Chou, S. C., Collins, W., Cox, P., Driouech, F., Emori, S., and Eyring, V.: Evaluation of climate models, in: Climate change 2013: the physical science basis.

Contribution of Working Group I to the Fifth Assessment Report of the Intergovernmental Panel on Climate Change, Cambridge University Press, 741-866, 2014.

Fleitmann, D., Cheng, H., Badertscher, S., Edwards, R. L., Mudelsee, M., Göktürk, O. M., Fankhauser, A., Pickering, R., Raible, C. C., Matter, A., Kramers, J., and Tüysüz, O.: Timing and climatic impact of Greenland interstadials recorded in stalagmites from northern Turkey, Geophysical Research Letters, 36, L19707-L19707, 10.1029/2009GL040050, 2009.

Göktürk, O. M., Fleitmann, D., Badertscher, S., Cheng, H., Edwards, R. L., Leuenberger, M., Fankhauser, A., Tüysüz, O., and Kramers, J.: Climate on the southern Black Sea coast during the Holocene: implications from the Sofular Cave record, Quaternary Science Reviews, 30, 2433-2445, https://doi.org/10.1016/J.QUASCIREV.2011.05.007, 2011.

Gordon, D., Smart, P. L., Ford, D. C., Andrews, J. N., Atkinson, T. C., Rowe, P. J., and Christopher, N. S. J.: Dating of late Pleistocene interglacial and interstadial periods in the United Kingdom from speleothem growth frequency, Quaternary Research, 31, 14-26, https://doi.org/10.1016/0033-5894(89)90082-3, 1989.

Grossman, E. L., and Ku, T.-L.: Oxygen and carbon isotope fractionation in biogenic aragonite: Temperature effects, Chemical Geology: Isotope Geoscience section, 59, 59-74, https://doi.org/10.1016/0168-9622(86)90057-6, 1986.

Hagemann, S., Arpe, K., and Roeckner, E.: Evaluation of the Hydrological Cycle in the ECHAM5 Model, Journal of Climate, 19, 3810-3827, https://doi.org/10.1175/JCLI3831.1, 2006.

Harris, I., Jones, P. D., Osborn, T. J., and Lister, D. H.: Updated high-resolution grids of monthly climatic observations – the CRU TS3.10 Dataset, International Journal of Climatology, 34, 623-642, https://doi.org/10.1002/joc.3711, retrieved from https://crudata.uea.ac.uk/cru/data/hrg/cru_ts_4.01/ on November 2018, , 2014.

Harrison, S. P., Bartlein, P. J., Brewer, S., Prentice, I. C., Boyd, M., Hessler, I., Holmgren, K., Izumi, K., and Willis, K.: Climate model benchmarking with glacial and mid-Holocene climates, Climate Dynamics, 43, 671-688, https://doi.org/10.1007/s00382-013-1922-6, 2014.

Harrison, S. P., Bartlein, P. J., Izumi, K., Li, G., Annan, J., Hargreaves, J., Braconnot, P., and Kageyama, M.: Evaluation of CMIP5 palaeo-simulations to improve climate projections, Nature Climate Change, 5, 735, 10.1038/nclimate2649

https://www.nature.com/articles/nclimate2649#supplementary-information, 2015.

Hartmann, A., Eiche, E., Neumann, T., Fohlmeister, J., Schröder-Ritzrau, A., Mangini, A., and Haryono, E.: Multi-proxy evidence for human-induced deforestation and cultivation from a late Holocene

stalagmite from middle Java, Indonesia, Chemical Geology, 357, 8-17, 10.1016/J.CHEMGEO.2013.08.026, 2013.

Hartmann, A., and Baker, A.: Modelling karst vadose zone hydrology and its relevance for paleoclimate reconstruction, Earth-Science Reviews, 172, 178-192, https://doi.org/10.1016/j.earscirev.2017.08.001, 2017.

Hendy, C. H., and Wilson, A. T.: Palaeoclimatic Data from Speleothems, Nature, 219, 48-51, https://doi.org/10.1038/219048a0, 1968.

Hessler, I., Harrison, S. P., Kucera, M., Waelbroeck, C., Chen, M. T., Anderson, C., de Vernal, A., Fréchette, B., Cloke-Hayes, A., Leduc, G., and Londeix, L.: Implication of methodological uncertainties for mid-Holocene sea surface temperature reconstructions, Clim. Past, 10, 2237-2252, https://doi.org/10.5194/cp-10-2237-2014, 2014.

Hoffmann, G., Werner, M., and Heimann, M.: Water isotope module of the ECHAM atmospheric general circulation model: A study on timescales from days to several years, Journal of Geophysical Research: Atmospheres, 103, 16871-16896, 1998.

Hoffmann, G., Jouzel, J., and Masson, V.: Stable water isotopes in atmospheric general circulation models, Hydrological Processes, 14, 1385-1406, https://doi.org/10.1002/1099-1085(20000615)14:8<1385::AID-HYP989>3.0.CO;2-1, 2000.

Hopcroft, P. O., Valdes, P. J., Woodward, S., and Joshi, M. M.: Last glacial maximum radiative forcing from mineral dust aerosols in an Earth system model, Journal of Geophysical Research: Atmospheres, 120, 8186-8205, 10.1002/2015jd023742, 2015.

Hu, J., Emile-Geay, J., Nusbaumer, J., and Noone, D.: Impact of Convective Activity on Precipitation δ18O in Isotope-Enabled General Circulation Models, Journal of Geophysical Research: Atmospheres, 123, 13,595-513,610, https://doi.org/10.1029/2018JD029187, 2018.

Jasechko, S., Lechler, A., Pausata, F. S. R., Fawcett, P. J., Gleeson, T., Cendón, D. I., Galewsky, J., LeGrande, A. N., Risi, C., Sharp, Z. D., Welker, J. M., Werner, M., and Yoshimura, K.: Late-glacial to late-Holocene shifts in global precipitation δ¹⁸O, Clim. Past, 11, 1375-1393, https://doi.org/10.5194/cp-11-1375-2015, 2015.

Jo, K. N., Woo, K. S., Yi, S., Yang, D. Y., Lim, H. S., Wang, Y. J., Cheng, H., and Edwards, R. L.: Mid-latitude interhemispheric hydrologic seesaw over the past 550,000 years, Nature, 508, 378-+, https://doi.org/10.1038/nature13076, 2014.

Johnston, V. E., Borsato, A., Frisia, S., Spötl, C., Dublyansky, Y., Töchterle, P., Hellstrom, J. C., Bajo, P., Edwards, R. L., and Cheng, H.: Evidence of thermophilisation and elevation-dependent warming

during the Last Interglacial in the Italian Alps, Scientific Reports, 8, 2680-2680, 10.1038/s41598-018-21027-3, 2018.

Joussaume, S., Sadourny, R., and Jouzel, J.: A general circulation model of water isotope cycles in the atmosphere, Nature, 311, 24-29, https://doi.org/10.1038/311024a0, 1984.

Jouzel, J., Hoffmann, G., Koster, R. D., and Masson, V.: Water isotopes in precipitation:: data/model comparison for present-day and past climates, Quaternary Science Reviews, 19, 363-379, https://doi.org/10.1016/S0277-3791(99)00069-4, 2000.

Kageyama, M., Albani, S., Braconnot, P., Harrison, S. P., Hopcroft, P. O., Ivanovic, R. F., Lambert, F., Marti, O., Peltier, W. R., Peterschmitt, J. Y., Roche, D. M., Tarasov, L., Zhang, X., Brady, E. C., Haywood, A. M., LeGrande, A. N., Lunt, D. J., Mahowald, N. M., Mikolajewicz, U., Nisancioglu, K. H., Otto-Bliesner, B. L., Renssen, H., Tomas, R. A., Zhang, Q., Abe-Ouchi, A., Bartlein, P. J., Cao, J., Li, Q., Lohmann, G., Ohgaito, R., Shi, X., Volodin, E., Yoshida, K., Zhang, X., and Zheng, W.: The PMIP4 contribution to CMIP6 – Part 4: Scientific objectives and experimental design of the PMIP4-CMIP6 Last Glacial Maximum experiments and PMIP4 sensitivity experiments, Geosci. Model Dev., 10, 4035-4055, https://doi.org/10.5194/gmd-10-4035-2017, 2017.

Kageyama, M., Braconnot, P., Harrison, S. P., Haywood, A. M., Jungclaus, J. H., Otto-Bliesner, B. L., Peterschmitt, J. Y., Abe-Ouchi, A., Albani, S., Bartlein, P. J., Brierley, C., Crucifix, M., Dolan, A., Fernandez-Donado, L., Fischer, H., Hopcroft, P. O., Ivanovic, R. F., Lambert, F., Lunt, D. J., Mahowald, N. M., Peltier, W. R., Phipps, S. J., Roche, D. M., Schmidt, G. A., Tarasov, L., Valdes, P. J., Zhang, Q., and Zhou, T.: The PMIP4 contribution to CMIP6 – Part 1: Overview and over-arching analysis plan, Geosci. Model Dev., 11, 1033-1057, 10.5194/gmd-11-1033-2018, 2018.

Kashiwaya, K., Atkinson, T. C., and Smart, P. L.: Periodic variations in late pleistocene speleothem abundance in Britain, Quaternary Research, 35, 190-196, https://doi.org/10.1016/0033-5894(91)90066-E, 1991.

Kim, S.-T., and O'Neil, J. R.: Equilibrium and nonequilibrium oxygen isotope effects in synthetic carbonates, Geochimica et Cosmochimica Acta, 61, 3461-3475, https://doi.org/10.1016/S0016-7037(97)00169-5, 1997.

Kirtman, B., Power, S. B., Adedoyin, A. J., Boer, G. J., Bojariu, R., Camilloni, I., Doblas-Reyes, F., Fiore, A. M., Kimoto, M., and Meehl, G.: Near-term Climate Change: Projections and Predictability, in: Climate Change 2013 – The Physical Science Basis: Working Group I Contribution to the Fifth Assessment Report of the Intergovernmental Panel on Climate Change, edited by: Change, I. P. o. C., Cambridge University Press, Cambridge, 953-1020, 2013.

Lachniet, M. S.: Climatic and environmental controls on speleothem oxygen-isotope values, Quaternary Science Reviews, 28, 412-432, https://doi.org/10.1016/j.quascirev.2008.10.021, 2009.

Lachniet, M. S.: Are aragonite stalagmites reliable paleoclimate proxies? Tests for oxygen isotope time-series replication and equilibrium, GSA Bulletin, 127, 1521-1533, https://doi.org/10.1130/B31161.1, 2015.

Langebroek, P. M., Werner, M., and Lohmann, G.: Climate information imprinted in oxygen-isotopic composition of precipitation in Europe, Earth and Planetary Science Letters, 311, 144-154, https://doi.org/10.1016/j.epsl.2011.08.049, 2011.

Lauritzen, S.-E., and Lundberg, J.: Calibration of the speleothem delta function: an absolute temperature record for the Holocene in northern Norway, The Holocene, 9, 659-669, 10.1191/095968399667823929, 1999.

LeGrande, A. N., and Schmidt, G. A.: Ensemble, water isotope–enabled, coupled general circulation modeling insights into the 8.2 ka event, Paleoceanography, 23, https://doi.org/10.1029/2008PA001610, 2008.

LeGrande, A. N., and Schmidt, G. A.: Sources of Holocene variability of oxygen isotopes in paleoclimate archives, Climate of the Past, 5, 441-455, https://doi.org/10.5194/cp-5-441-2009, 2009.

Lundeen, Z., Brunelle, A., Burns, S. J., Polyak, V., and Asmerom, Y.: A speleothem record of Holocene paleoclimate from the northern Wasatch Mountains, southeast Idaho, USA, Quaternary International, 310, 83-95, https://doi.org/10.1016/J.QUAINT.2013.03.018, 2013.

Mangini, A., Blumbach, P., Verdes, P., Spötl, C., Scholz, D., Machel, H., and Mahon, S.: Combined records from a stalagmite from Barbados and from lake sediments in Haiti reveal variable seasonality in the Caribbean between 6.7 and 3 ka BP, Quaternary Science Reviews, 26, 1332-1343, 10.1016/J.QUASCIREV.2007.01.011, 2007.

MARGO project members: Constraints on the magnitude and patterns of ocean cooling at the Last Glacial Maximum, Nature Geoscience, 2, 127, https://doi.org/10.1038/ngeo411, 2009.

Marshall, D., Ghaleb, B., Countess, R., and Gabities, J.: Preliminary paleoclimate reconstruction based on a 12,500 year old speleothem from Vancouver Island, Canada: stable isotopes and U–Th disequilibrium dating, Quaternary Science Reviews, 28, 2507-2513, 10.1016/J.QUASCIREV.2009.05.019, 2009.

Mauri, A., Davis, B. A. S., Collins, P. M., and Kaplan, J. O.: The influence of atmospheric circulation on the mid-Holocene climate of Europe: a data–model comparison, Clim. Past, 10, 1925-1938, 10.5194/cp-10-1925-2014, 2014.

McDermott, F.: Palaeo-climate reconstruction from stable isotope variations in speleothems: a review, Quaternary Science Reviews, 23, 901-918, https://doi.org/10.1016/j.quascirev.2003.06.021, 2004.

McDermott, F., Atkinson, T. C., Fairchild, I. J., Baldini, L. M., and Mattey, D. P.: A first evaluation of the spatial gradients in delta O-18 recorded by European Holocene speleothems, Global and Planetary Change, 79, 275-287, https://doi.org/10.1016/j.gloplacha.2011.01.005, 2011.

Messori, G., Gaetani, M., Zhang, Q., Zhang, Q., and Pausata, F. S. R.: The water cycle of the mid-Holocene West African monsoon: The role of vegetation and dust emission changes, International Journal of Climatology, 39, 1927-1939, 10.1002/joc.5924, 2019.

Mickler, P. J., Banner, J. L., Stern, L., Asmerom, Y., Edwards, R. L., and Ito, E.: Stable isotope variations in modern tropical speleothems: Evaluating equilibrium vs. kinetic isotope effects, Geochimica et Cosmochimica Acta, 68, 4381-4393, https://doi.org/10.1016/J.GCA.2004.02.012, 2004.

Mickler, P. J., Stern, L. A., and Banner, J. L.: Large kinetic isotope effects in modern speleothems, Geological Society of America Bulletin, 118, 65-81, https://doi.org/10.1130/B25698.1, 2006.

Moore, G. W., and Sullivan, N.: Spelology Caves and the Cave Environment, 3rd Edition ed., Cave Books, St. Louis, 1997.

Myers, C. G., Oster, J. L., Sharp, W. D., Bennartz, R., Kelley, N. P., Covey, A. K., and Breitenbach, S. F. M.: Northeast Indian stalagmite records Pacific decadal climate change: Implications for moisture transport and drought in India, Geophysical Research Letters, 42, 4124-4132, https://doi.org/10.1002/2015GL063826, 2015.

Nagra, G., Treble, P. C., Andersen, M. S., Bajo, P., Hellstrom, J., and Baker, A.: Dating stalagmites in mediterranean climates using annual trace element cycles, Scientific Reports, 7, https://doi.org/10.1038/s41598-017-00474-4, 2017.

Noone, D., and Simmonds, I.: Associations between δ18O of Water and Climate Parameters in a Simulation of Atmospheric Circulation for 1979–95, Journal of Climate, 15, 3150-3169, https://doi.org/10.1175/1520-0442(2002)015<3150:aboowa>2.0.co;2, 2002.

Novello, V. F., Cruz, F. W., Vuille, M., Stríkis, N. M., Edwards, R. L., Cheng, H., Emerick, S., de Paula, M. S., Li, X., Barreto, E. d. S., Karmann, I., and Santos, R. V.: A high-resolution history of the South American Monsoon from Last Glacial Maximum to the Holocene, Scientific Reports, 7, 44267-44267, https://doi.org/10.1038/srep44267, 2017.

Novello, V. F., Cruz, F. W., Moquet, J. S., Vuille, M., de Paula, M. S., Nunes, D., Edwards, R. L., Cheng, H., Karmann, I., Utida, G., Stríkis, N. M., and Campos, J. L. P. S.: Two Millennia of South Atlantic

Convergence Zone Variability Reconstructed From Isotopic Proxies, Geophysical Research Letters, 45, 5045-5051, https://doi.org/10.1029/2017GL076838, 2018.

Oster, J. L., Montañez, I. P., Mertz-Kraus, R., Sharp, W. D., Stock, G. M., Spero, H. J., Tinsley, J., and Zachos, J. C.: Millennial-scale variations in western Sierra Nevada precipitation during the last glacial cycle MIS 4/3 transition, Quaternary Research, 82, 236-248, https://doi.org/10.1016/j.yqres.2014.04.010, 2014.

Oster, J. L., Sharp, W. D., Covey, A. K., Gibson, J., Rogers, B., and Mix, H.: Climate response to the 8.2 ka event in coastal California, Scientific Reports, 7, 3886-3886, https://doi.org/10.1038/s41598-017-04215-5, 2017.

Partin, J. W., Cobb, K. M., Adkins, J. F., Clark, B., and Fernandez, D. P.: Millennial-scale trends in west Pacific warm pool hydrology since the Last Glacial Maximum, Nature, 449, 452-455, https://doi.org/10.1038/nature06164, 2007.

Paul, A., and Schäfer-Neth, C.: Modeling the water masses of the Atlantic Ocean at the Last Glacial Maximum, Paleoceanography, 18, https://doi.org/10.1029/2002PA000783, 2003.

Perez-Sanz, A., Li, G., González-Sampériz, P., and Harrison, S. P.: Evaluation of modern and mid-Holocene seasonal precipitation of the Mediterranean and northern Africa in the CMIP5 simulations, Clim. Past, 10, 551-568, https://doi.org/10.5194/cp-10-551-2014, 2014.

Pollock, A. L., van Beynen, P. E., DeLong, K. L., Polyak, V., Asmerom, Y., and Reeder, P. P.: A mid-Holocene paleoprecipitation record from Belize, Palaeogeography, Palaeoclimatology, Palaeoecology, 463, 103-111, https://doi.org/10.1016/J.PALAEO.2016.09.021, 2016.

Qian, Y., Jackson, C., Giorgi, F., Booth, B., Duan, Q., Forest, C., Higdon, D., Hou, Z. J., and Huerta, G.: Uncertainty Quantification in Climate Modeling and Projection, Bulletin of the American Meteorological Society, 97, 821-824, 10.1175/BAMS-D-15-00297.1, 2016.

Riechelmann, S., Schroder-Ritzrau, A., Spotl, C., Riechelmann, D. F. C., Richter, D. K., Mangini, A., Frank, N., Breitenbach, S. F. M., and Immenhauser, A.: Sensitivity of Bunker Cave to climatic forcings highlighted through multi-annual monitoring of rain-, soil-, and dripwaters, Chemical Geology, 449, 194-205, https://doi.org/10.1016/j.chemgeo.2016.12.015, 2017.

Risi, C., Ogée, J., Bony, S., Bariac, T., Raz-Yaseef, N., Wingate, L., Welker, J., Knohl, A., Kurz-Besson, C., Leclerc, M., Zhang, G., Buchmann, N., Santrucek, J., Hronkova, M., David, T., Peylin, P., and Guglielmo, F.: The Water Isotopic Version of the Land-Surface Model ORCHIDEE: Implementation, Evaluation, Sensitivity to Hydrological Parameters, Hydrology: Current Research, 7, https://doi.org/10.4172/2157-7587.1000258, 2016.

Roche, D. M.: δ18O water isotope in the iLOVECLIM model (version 1.0) – Part 1: Implementation and verification, Geosci. Model Dev., 6, 1481-1491, https://doi.org/10.5194/gmd-6-1481-2013, 2013.

Roeckner, E., Baeuml, G., Bonaventura, L., Brokopf, R., Esch, M., Giorgetta, M., Hagemann, S., Kirchner, I., Kornblueh, L., Manzini, E., Rhodin, A., Schlese, U., Schulzweida, U., and Tompkins, A.: The general circulation model ECHAM5. Part I: Model description, Max Planck Institute for Meteorology, Hamburg 349, 140, 2003.

Roeckner, E., Brokopf, R., Esch, M., Giorgetta, M., Hagemann, S., Kornblueh, L., Manzini, E., Schlese, U., and Schulzweida, U.: Sensitivity of Simulated Climate to Horizontal and Vertical Resolution in the ECHAM5 Atmosphere Model, Journal of Climate, 19, 3771-3791, https://doi.org/10.1175/jcli3824.1, 2006.

Rowe, P. J., Mason, J. E., Andrews, J. E., Marca, A. D., Thomas, L., van Calsteren, P., Jex, C. N., Vonhof, H. B., and Al-Omari, S.: Speleothem isotopic evidence of winter rainfall variability in northeast Turkey between 77 and 6 ka, Quaternary Science Reviews, 45, 60-72, https://doi.org/10.1016/J.QUASCIREV.2012.04.013, 2012.

Schmidt, G. A., LeGrande, A. N., and Hoffmann, G.: Water isotope expressions of intrinsic and forced variability in a coupled ocean-atmosphere model, Journal of Geophysical Research: Atmospheres, 112, https://doi.org/10.1029/2006JD007781, 2007.

Schmidt, G. A., Annan, J. D., Bartlein, P. J., Cook, B. I., Guilyardi, E., Hargreaves, J. C., Harrison, S. P., Kageyama, M., LeGrande, A. N., Konecky, B., Lovejoy, S., Mann, M. E., Masson-Delmotte, V., Risi, C., Thompson, D., Timmermann, A., Tremblay, L. B., and Yiou, P.: Using palaeo-climate comparisons to constrain future projections in CMIP5, Clim. Past, 10, 221-250, https://doi.org/10.5194/cp-10-221-2014, 2014.

Scroxton, N., Gagan, M. K., Dunbar, G. B., Ayliffe, L. K., Hantoro, W. S., Shen, C.-C., Hellstrom, J. C., Zhao, J.-x., Cheng, H., Edwards, R. L., Sun, H., and Rifai, H.: Natural attrition and growth frequency variations of stalagmites in southwest Sulawesi over the past 530,000years, Palaeogeography, Palaeoclimatology, Palaeoecology, 441, 823-833, https://doi.org/10.1016/j.palaeo.2015.10.030, 2016.

Sharp, Z.: Principles of stable isotope geochemistry, 1st ed., Pearson Education, Upper Saddler River, N.J., 2007.

Stinnesbeck, W., Becker, J., Hering, F., Frey, E., González, A. G., Fohlmeister, J., Stinnesbeck, S., Frank, N., Terrazas Mata, A., Benavente, M. E., Avilés Olguín, J., Aceves Núñez, E., Zell, P., and Deininger,

M.: The earliest settlers of Mesoamerica date back to the late Pleistocene, PLOS ONE, 12, e0183345-e0183345, 10.1371/journal.pone.0183345, 2017.

Sundqvist, H. S., Holmgren, K., and Lauritzen, S. E.: Stable isotope variations in stalagmites from northwestern Sweden document climate and environmental changes during the early Holocene, The Holocene, 17, 259-267, https://doi.org/10.1177/0959683607073292, 2007.

Swann, A. L. S., Fung, I. Y., Liu, Y., and Chiang, J. C. H.: Remote Vegetation Feedbacks and the Mid-Holocene Green Sahara, Journal of Climate, 27, 4857-4870, 10.1175/jcli-d-13-00690.1, 2014.

Tindall, J. C., Valdes, P. J., and Sime, L. C.: Stable water isotopes in HadCM3: Isotopic signature of El Niño–Southern Oscillation and the tropical amount effect, Journal of Geophysical Research: Atmospheres, 114, https://doi.org/10.1029/2008JD010825, 2009.

Treble, P., Shelley, J. M. G., and Chappell, J.: Comparison of high resolution sub-annual records of trace elements in a modern (1911–1992) speleothem with instrumental climate data from southwest Australia, Earth and Planetary Science Letters, 216, 141-153, https://doi.org/10.1016/S0012-821X(03)00504-1, 2003.

Treble, P. C., Chappell, J., Gagan, M. K., McKeegan, K. D., and Harrison, T. M.: In situ measurement of seasonal delta O-18 variations and analysis of isotopic trends in a modem speleothem from southwest Australia, Earth and Planetary Science Letters, 233, 17-32, https://doi.org/10.1016/j.epsl.2005.02.013, 2005.

Treble, P. C., Baker, A., Ayliffe, L. K., Cohen, T. J., Hellstrom, J. C., Gagan, M. K., Frisia, S., Drysdale, R. N., Griffiths, A. D., and Borsato, A.: Hydroclimate of the Last Glacial Maximum and deglaciation in southern Australia's arid margin interpreted from speleothem records (23-15 ka), Climate of the Past, 13, 667-687, https://doi.org/10.5194/cp-13-667-2017, 2017.

Tremaine, D. M., Froelich, P. N., and Wang, Y.: Speleothem calcite farmed in situ: Modern calibration of δ18O and δ13C paleoclimate proxies in a continuously-monitored natural cave system, Geochimica et Cosmochimica Acta, 75, 4929-4950, https://doi.org/10.1016/j.gca.2011.06.005, 2011.

Vaks, A., Bar-Matthews, M., Ayalon, A., Matthews, A., Frumkin, A., Dayan, U., Halicz, L., Almogi-Labin, A., and Schilman, B.: Paleoclimate and location of the border between Mediterranean climate region and the Saharo-Arabian Desert as revealed by speleothems from the northern Negev Desert, Israel, Earth and Planetary Science Letters, 249, 384-399, https://doi.org/10.1016/j.epsl.2006.07.009, 2006.

Vaks, A., Gutareva, O. S., Breitenbach, S. F. M., Avirmed, E., Mason, A. J., Thomas, A. L., Osinzev, A. V., Kononov, A. M., and Henderson, G. M.: Speleothems Reveal 500,000-Year History of Siberian Permafrost, Science, 340, 183-186, https://doi.org/10.1126/science.1228729, 2013.

Vanghi, V., Borsato, A., Frisia, S., Drysdale, R., Hellstrom, J., and Bajo, P.: Climate variability on the Adriatic seaboard during the last glacial inception and MIS 5c from Frasassi Cave stalagmite record, Quaternary Science Reviews, 201, 349-361, https://doi.org/10.1016/J.QUASCIREV.2018.10.023, 2018.

Wackerbarth, A., Langebroek, P. M., Werner, M., Lohmann, G., Riechelmann, S., Borsato, A., and Mangini, A.: Simulated oxygen isotopes in cave drip water and speleothem calcite in European caves, Climate of the Past, 8, 1781-1799, https://doi.org/10.5194/cp-8-1781-2012, 2012.

Wang, X., Edwards, R. L., Auler, A. S., Cheng, H., Kong, X., Wang, Y., Cruz, F. W., Dorale, J. A., and Chiang, H.-W.: Hydroclimate changes across the Amazon lowlands over the past 45,000 years, Nature, 541, 204-207, https://doi.org/10.1038/nature20787, 2017.

Wang, Y., Cheng, H., Edwards, R. L., He, Y., Kong, X., An, Z., Wu, J., Kelly, M. J., Dykoski, C. A., and Li, X.: The Holocene Asian monsoon: links to solar changes and North Atlantic climate, Science (New York, N.Y.), 308, 854-857, https://doi.org/10.1126/science.1106296, 2005.

Waterisotopes Database: http://waterisotopes.org. Accessed 04/2017. Query: type=Precipitation, 2017.

Werner, M., Langebroek, P. M., Carlsen, T., Herold, M., and Lohmann, G.: Stable water isotopes in the ECHAM5 general circulation model: Toward high-resolution isotope modeling on a global scale, Journal of Geophysical Research: Atmospheres, 116, https://doi.org/10.1029/2011JD015681, 2011.

Werner, M., Haese, B., Xu, X., Zhang, X., Butzin, M., and Lohmann, G.: Glacial-interglacial changes in (H2O)-O-18, HDO and deuterium excess - results from the fully coupled ECHAM5/MPI-OM Earth system model, Geoscientific Model Development, 9, 647-670, https://doi.org/10.5194/gmd-9-647-2016, 2016.

Werner, M., Jouzel, J., Masson-Delmotte, V., and Lohmann, G.: Reconciling glacial Antarctic water stable isotopes with ice sheet topography and the isotopic paleothermometer, Nature Communications, 9, 3537, https://doi.org/10.1038/s41467-018-05430-y, 2018.

Winter, A., Zanchettin, D., Miller, T., Kushnir, Y., Black, D., Lohmann, G., Burnett, A., Haug, G. H., Estrella-Martínez, J., Breitenbach, S. F. M., Beaufort, L., Rubino, A., and Cheng, H.: Persistent drying

in the tropics linked to natural forcing, Nature Communications, 6, 7627-7627, https://doi.org/10.1038/ncomms8627, 2015.

Wolff, C., Plessen, B., Dudashvilli, A. S., Breitenbach, S. F. M., Cheng, H., Edwards, L. R., and Strecker, M. R.: Precipitation evolution of Central Asia during the last 5000 years, The Holocene, 27, 142-154, 10.1177/0959683616652711, 2017.

Wurtzel, J. B., Abram, N. J., Lewis, S. C., Bajo, P., Hellstrom, J. C., Troitzsch, U., and Heslop, D.: Tropical Indo-Pacific hydroclimate response to North Atlantic forcing during the last deglaciation as recorded by a speleothem from Sumatra, Indonesia, Earth and Planetary Science Letters, 492, 264-278, https://doi.org/10.1016/J.EPSL.2018.04.001, 2018.

Xi, X.: A Review of Water Isotopes in Atmospheric General Circulation Models: Recent Advances and Future Prospects, International Journal of Atmospheric Sciences, 2014, 16, https://doi.org/10.1155/2014/250920, 2014.

Xia, Q. K., Zhao, J. X., and Collerson, K. D.: Early-Mid Holocene climatic variations in Tasmania, Australia: multi-proxy records in a stalagmite from Lynds Cave, Earth and Planetary Science Letters, 194, 177-187, https://doi.org/10.1016/s0012-821x(01)00541-6, 2001.

Yonge, C. J., Ford, D. C., Gray, J., and Schwarcz, H. P.: Stable isotope studies of cave seepage water, Chemical Geology: Isotope Geoscience section, 58, 97-105, https://doi.org/10.1016/0168-9622(85)90030-2, 1985.

Yoshimori, M., Yokohata, T., and Abe-Ouchi, A.: A Comparison of Climate Feedback Strength between CO2 Doubling and LGM Experiments, Journal of Climate, 22, 3374-3395, 10.1175/2009jcli2801.1, 2009.

Zhu, J., Liu, Z. Y., Brady, E. C., Otto-Bliesner, B. L., Marcott, S. A., Zhang, J. X., Wang, X. F., Nusbaumer, J., Wong, T. E., Jahn, A., and Noone, D.: Investigating the Direct Meltwater Effect in Terrestrial Oxygen-Isotope Paleoclimate Records Using an Isotope-Enabled Earth System Model, Geophysical Research Letters, 44, 12501-12510, https://doi.org/10.1002/2017gl076253, 2017.

18 Figures

Figure 1: Spatio-temporal distribution of SISALv1b database. **(a)** Spatial distribution of speleothem records. Filled circles are sites used in this study (SISALv1 in ~~purple~~blue; SISALv1b in ~~light blue~~green). ~~Crosses~~ Triangles are SISAL sites that do not pass the screening described in section 2.3 and/or do not cover the time periods used here (modern, MH and LGM). The background carbonate lithology is that of the World Karst Aquifer Mapping (WOKAM) project (Chen et al., 2017). **(b)** Temporal distribution of speleothem records according to regions. The non-overlapping bins span 1,000 years and start on 1950 CE. Regions have been defined as: Oceania (-60° < Lat < 0°; 90° < Lon < 180°); Asia (0° < Lat < 60°; 60° < Lon < 130°); Middle East (7.6° < Lat < 50°; 26° < Lon < 59°); Africa (-45° < Lat < 36.1°; -30° < Lon < 60°; with records in the Middle East region removed); Europe (36.7° < Lat < 75°; -30° < Lon < 30°; plus Gibraltar and Siberian sites); South America (-60° < Lat < 8°; -150° < Lon < -30°); North and Central America (8.1° < Lat < 60°; -150° < Lon < -50°).

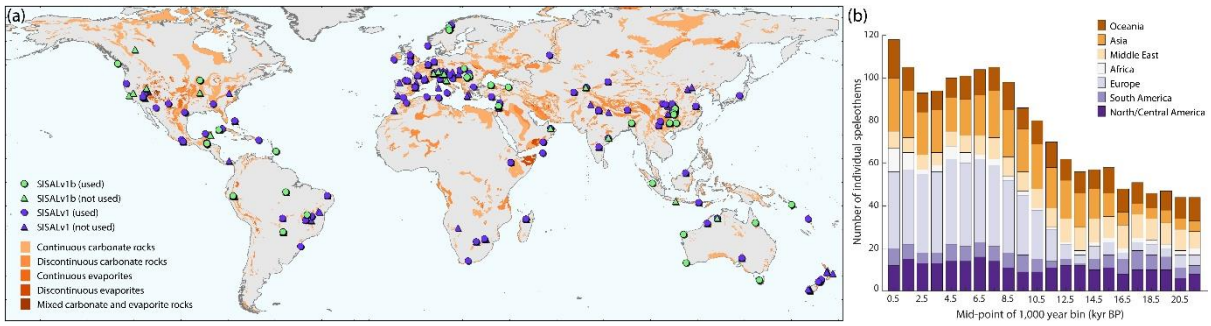

Figure 2: Distribution of the number of ~~unique~~ single caves with speleothem growth through time. (**a)** Number of ~~unique~~ single caves with growth over the last 500,000 yrs BP (where present is 1950 CE) in 1000-year bins (solid line), bootstrapped estimate of uncertainty (shading between 5 and 95% percentiles) and fitted exponential distribution (darker solid line). Horizontal bars denote previous interglacials. (**b, c**) same as a) but with the fitted exponential distribution subtracted to highlight anomalies from the expected number of caves over the last 300 kyrs BP. Horizontal bars ~~in b) and c)~~ indicate periods with significantly greater (dark grey) or fewer (light grey) number of caves with speleothem growth than expected. Green indicates the full global dataset, blue and red indicate temperate and tropical subdivisions respectively. ~~Horizontal bars in a) denote previous interglacials.~~

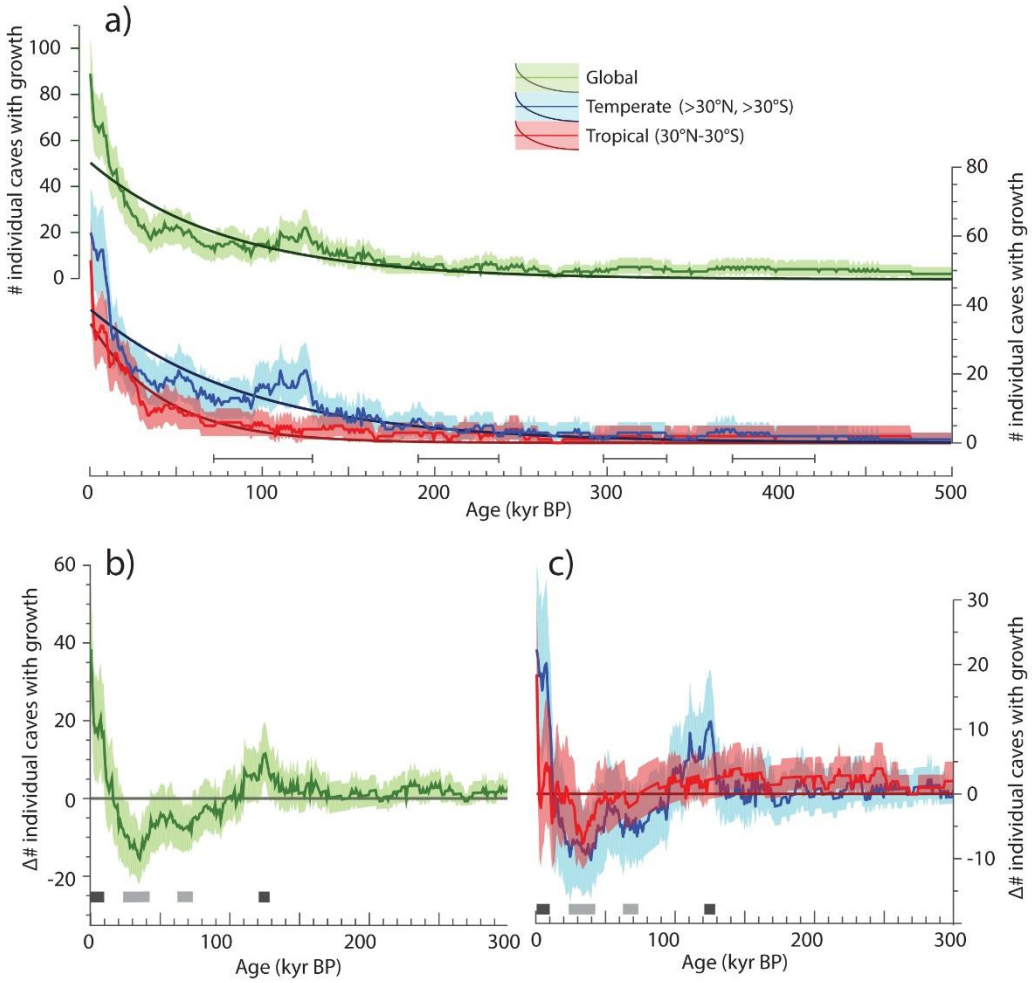

1240 **Figure 3:** Comparison of SISAL data with observational and simulated $w\delta^{18}O_p$ for the modern period. **(a)** Comparison between SISAL $\delta^{18}O$ averages [‰; V-SMOW] for the period 1960–2017 CE with OIPC data [‰; V-SMOW]. **(b)** Scatterplot of SISAL modern $\delta^{18}O$ averages as in (a) versus $w\delta^{18}O_p$ extracted from OIPC (i.e., background map in (a)) at the location of each cave site. **(c)** Same ~~than~~ as (a) with simulated $w\delta^{18}O_p$ data for the period 1958–2013 in the background. **(d)** Scatterplot of SISAL 1245 modern $\delta^{18}O$ as in (c) versus the simulated $w\delta^{18}O_p$ for the period 1958–2013 CE. Dashed lines in (b) and (d) represent~~s~~ the 1:1 line. All SISAL isotope data have been converted to their drip-water equivalent, following the approach described in section 3.2. ~~using the calcite-water $\delta^{18}O$ fractionation equation from Tremaine et al. (2011)~~. Mean annual air surface temperature from CRU-TS4.01 (Harris et al., 2014) and mean annual simulated ECHAM5-wiso air surface temperature were used as 1250 surrogates for cave temperatures in the OIPC and ECHAM5-wiso comparison, respectively. See section 2.3 for details on data extraction and conversion.

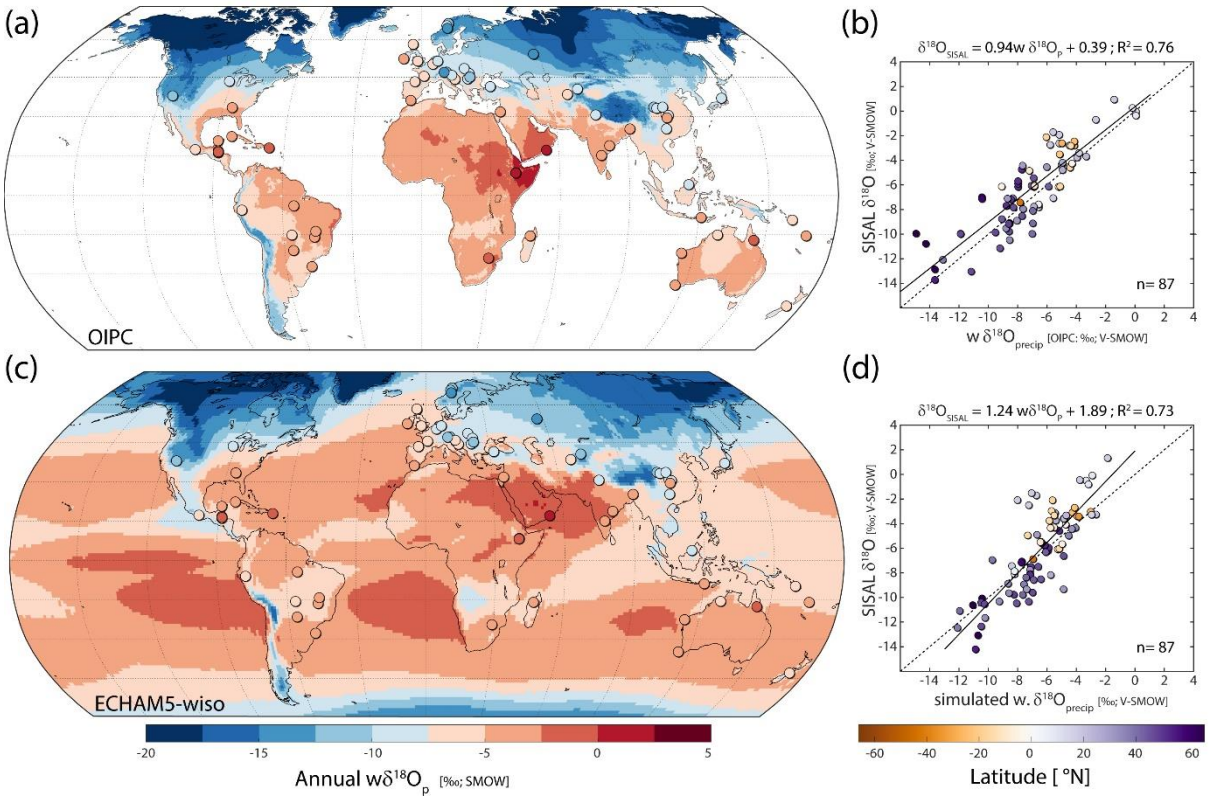

Figure ~~43~~: Modern global inter-annual $\delta^{18}O$ variability. Box plots show the variability of the standard deviation of global annual w$\delta^{18}O$ using: **(left)** GNIP stations with enough months of data to account for >80% of the annual precipitation ~~at least 10 months of data per year~~ and at least 5 years of data (n = 450) and ECHAM5-wiso data extracted at the location of each GNIP station for the years when this data is available; **(right)** SISAL records with at least 5 isotope samples for the period 1958–2013 and simulated w$\delta^{18}O_p$ extracted at each cave location for the same years for which speleothem data is available. Boxplots in shades of red ~~at the rightmost of the panel~~ are constructed after smoothing the simulated w$\delta^{18}O_p$ data for 1 to 16 years. On each box, the central ~~red~~ mark indicates the median (q_2; 50th percentile) and the bottom and top edges of the box indicate the 25th (q_1) and 75th (q_3) percentiles, respectively. Outliers (~~red~~ black crosses) are locations with standard deviations greater than $q_3 + 1.5 \times (q_3 - q_1)$ or less than $q_1 - 1.5 \times (q_3 - q_1)$. This corresponds to approximately ±2.7σ or 99.3% coverage if the data are normally distributed. If the notches in the box plots do not overlap, you can conclude, with 95% confidence, that the true medians do differ. The grey horizontal band corresponds to the notch in SISAL for easy comparison. SISAL data were converted to their drip-water $\delta^{18}O$ equivalent as described in section 2.3.

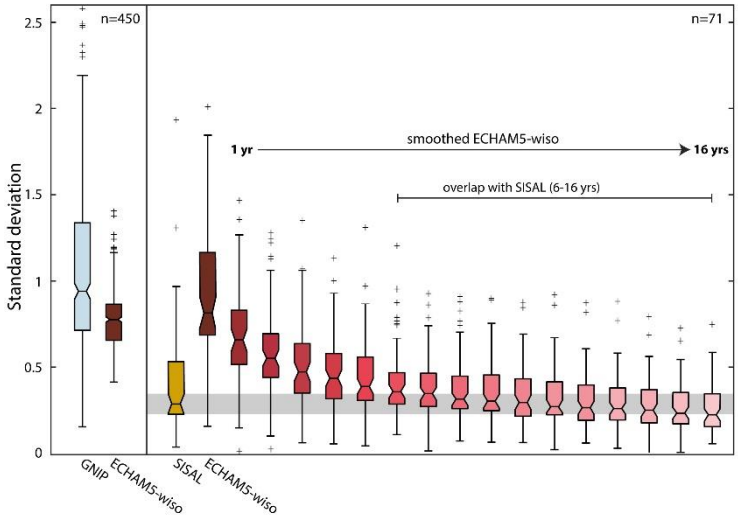

Figure 5: ECHAM5-wiso weighted $\delta^{18}O_p$ anomalies ([‰; V-SMOW]; background map) and SISAL isotope anomalies ([‰; V-~~PDB~~SMOW]; filled circles) for three time-slices: **(a)** MH-PI (SISAL records n = 3~~6~~4), **(b)** LGM-PI (SISAL records n = 1~~3~~1) and **(c)** LGM-MH (SISAL records n = 2~~0~~0). For easy visualisation, when there are two speleothem records from the same cave site, one has been shifted 2° towards the North and the East (shown here as triangles). Note the different colour bar axis in the colour bar of (a) compared to (b) and (c). Two-tailed student t-test has been applied to calculate the significance of the ECHAM5-wiso anomalies in (a) and (b) at a 95% confidence. No significance has been calculated for (c), which compares two different simulations with their corresponding control periods. SISAL anomalies calculated with respect to 1850–1990 CE. Small black crosses indicate SISAL entities that do not have a modern equivalent. SISAL data has been converted to its drip water equivalent prior to calculating the anomalies as described in section 2.3.

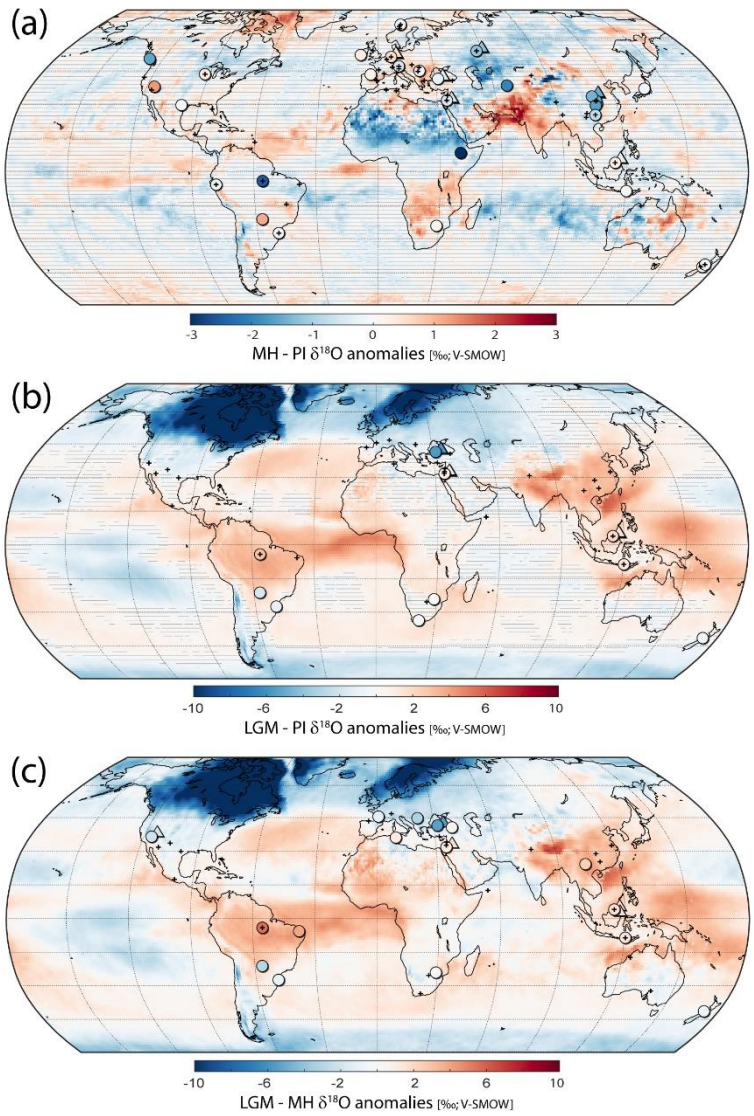

Figure 6: LGM period definitions and their impact on SISAL $\delta^{18}O$ mean estimate uncertainty. The impact of the window definition and age uncertainty is explored for two entities **(a)** entity BT-2 from Botuverá cave (Cruz et al., 2005) and **(b)** entity SSC01 from Gunung-buda cave (Partin et al., 2007). The relative error is defined as 2 standard deviations for the original age model and the COPRA median; and the upper minus lower 95% quantiles for the COPRA median uncertainty as well as the COPRA ensemble spread of standard deviations. Black solid lines give the relative error of the mean isotopic estimate for the LGM for the original age model and~~, the~~ grey solid lines give ~~for~~ the estimate based on the COPRA median age model. The pink dotted line shows the uncertainty of the COPRA median estimate, and the green dashed line the average relative error estimate across the 1,000-member COPRA ensemble. For both speleothems, relatively stable error estimates are found for window sizes larger than ±750 years, whereas the relative error increases towards smaller window sizes.

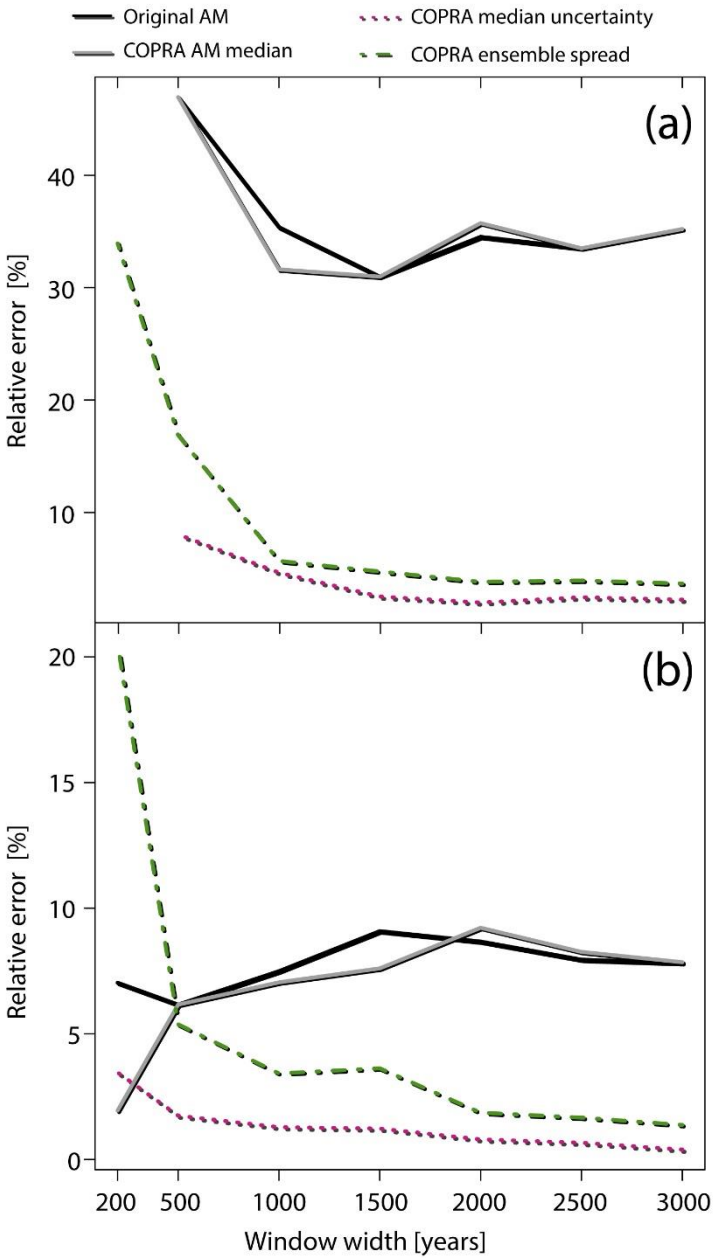

Figure 7: Latitudinal isotopic transect for Asia during the (a) Modern (1958-2013), (b) Mid-Holocene (MH; 6 ±0.5 kyrs BP) and (c) Last Glacial Maximum (LGM; 20 ±1 kyrs BP) periods. Background maps at the top of each panel show the simulated $w\delta^{18}O_p$ from ECHAM5-wiso. Bottom plots in each panel show the simulated $w\delta^{18}O_p$ data extracted for each transect: black circles and grey whiskers are mean ±2 standard deviation of the data extracted along longitudinal sections in between the two great circle lines shown in solid black lines in the top maps. The red line is the median of the extracted data. All data were extracted at steps of 1.12° to coincide with the average model grid-size. These bottom panels also show SISAL $\delta^{18}O$: circles for low-elevation sites, < 1,000 masl; triangles for high-elevation sites, > 1,000 masl. ~~Mid-Holocene (MH) transects for three regions: **(a)** NW to SE across North America; **(b)** N-S across southern Europe and northern Africa, and **(c)** NW to SE across SE Asia. Maps at the top~~

~~of each panel show the simulated $\delta^{18}O_p$ (left), Mean Annual Temperature (MAT; centre) and Mean Annual Precipitation (MAP; right) from ECHAM5-wiso. The same scale is used for the $\delta^{18}O$, MAT and MAP maps. All transects show absolute $\delta^{18}O$ values. In the $\delta^{18}O$ maps, filled circles are SISAL $\delta^{18}O$ averages for entities that cover both the MH and the modern reference period. Filled squares are SISAL entities that do not have a corresponding modern. Bottom plots of each panel show the simulated data extracted for each transect: black circles and whiskers are mean ±1 standard deviation of the data extracted along longitudinal sections in between the two great circle lines shown in solid grey lines in the top maps. The red line is the median of the extracted data. All data were extracted at steps of 1.12^o to coincide with the average model grid size. Bottom plots in each panel also show SISAL $\delta^{18}O$ (circles for low-elevation sites, < 1,000 masl; triangles for high-elevation sites, > 1,000 masl), pollen-based quantitative reconstructions of MAT (red squares; Bartlein et al., 2011) and MAP (blue squares; Bartlein et al., 2011). Pollen-based reconstructions have been converted to absolute values by adding the CRU TS4.01 climatology (Harris et al., 2014).~~

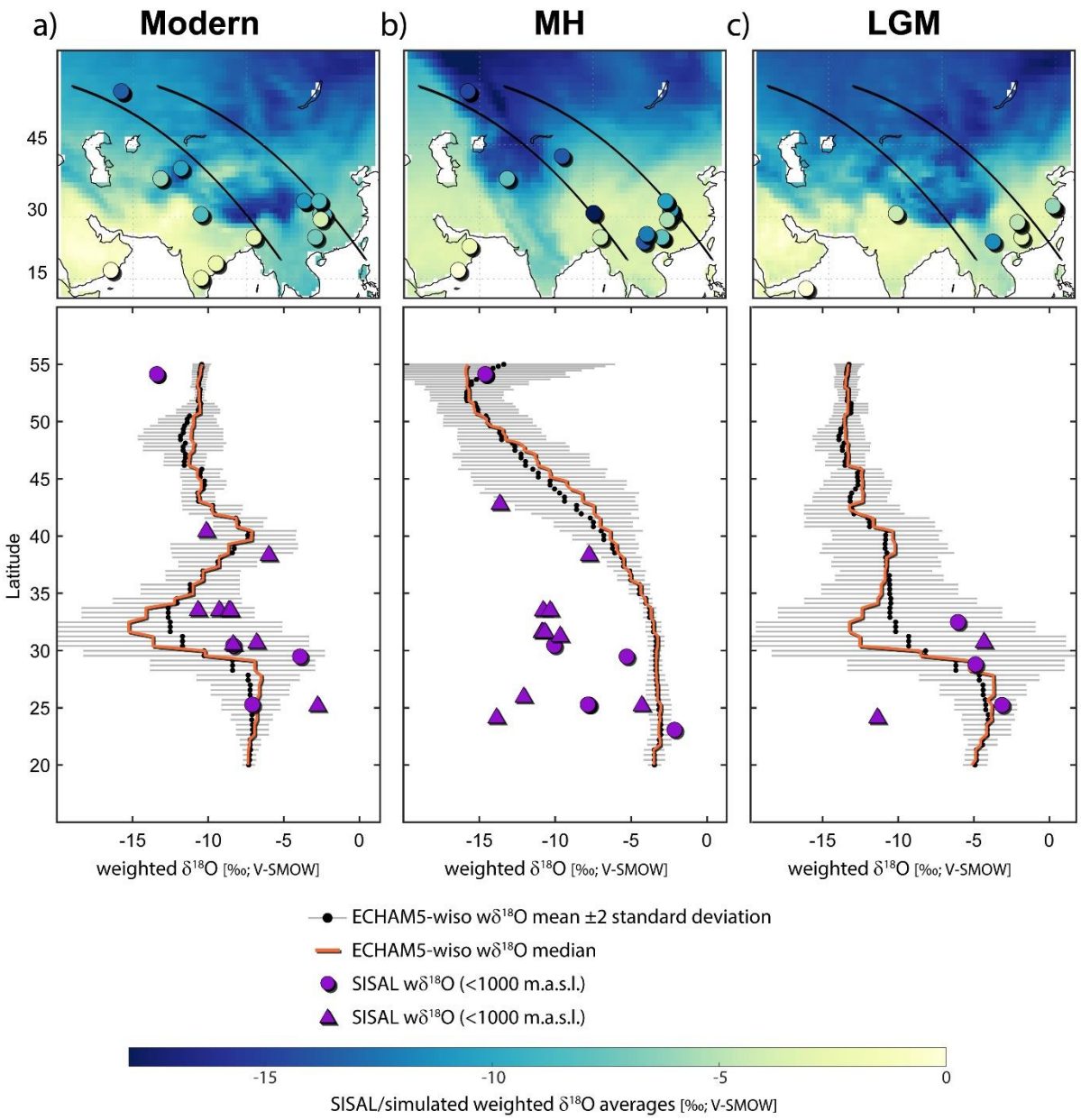

Figure 8: Longitudinal isotopic transect for Europe during the (a) Modern (1958-2013), (b) Mid-Holocene (MH; 6 ±0.5 kyrs BP) and (c) Last Glacial Maximum (LGM; 20 ±1 kyrs BP) periods. Details as in caption of Fig. 7. ~~Last Glacial Maximum (LGM) transects for three regions: **(a)** NW to SE across North America; **(b)** N-S from central Europe to southern Africa, and **(c)** NW-SE from China to northern Australia. Details as in caption of Fig. 7.~~

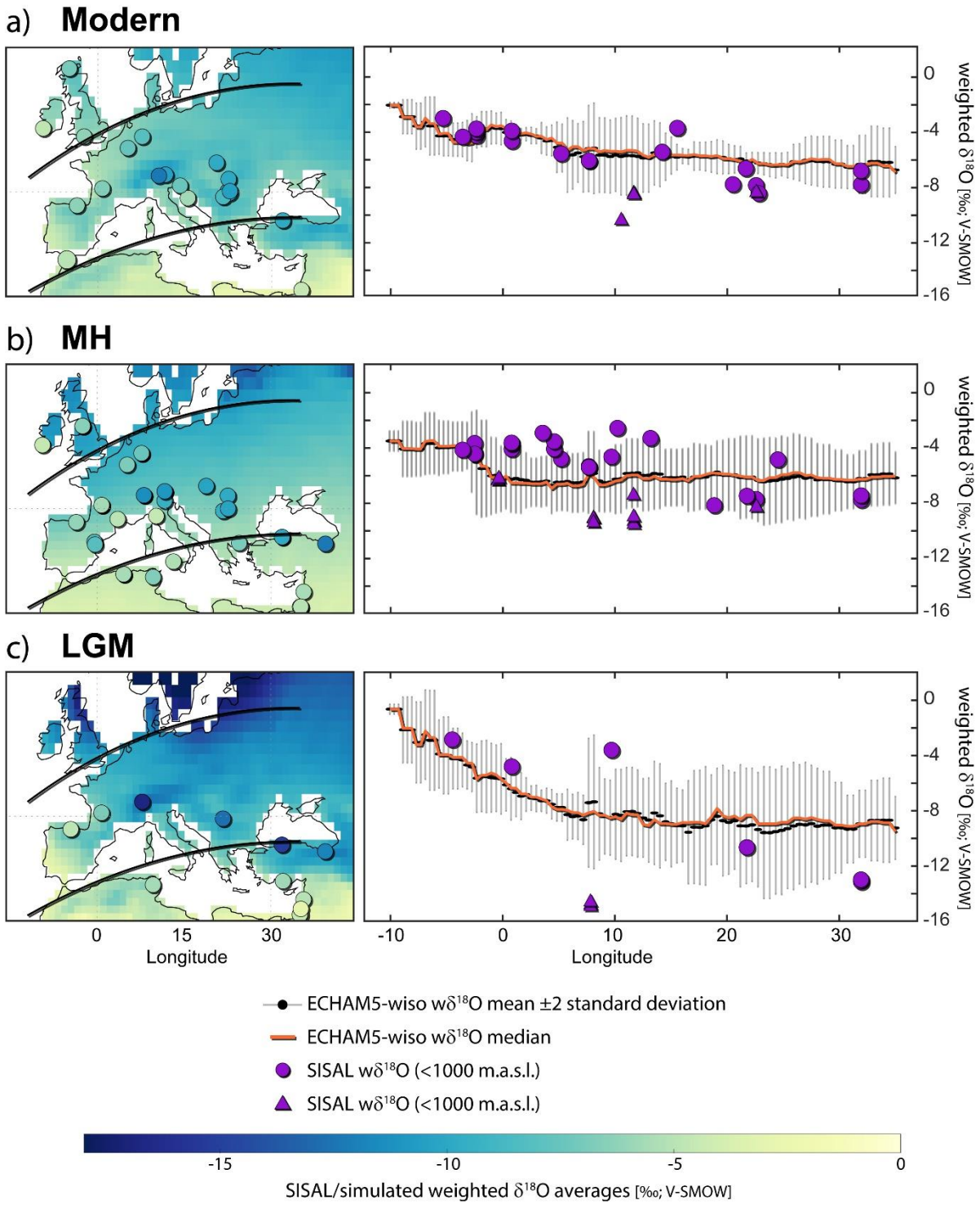

19 Tables

Table 1: List of speleothem records that have been added to SISALv1 (Atsawawaranunt et al., 2018a; Atsawawaranunt et al., 2018b) to produce SISALv1b (Atsawawaranunt et al., 2019) sorted alphabetically by site name. Elevation is in metres above sea level (masl), latitude in degrees North and longitude in degrees East.

Site name	Elev.	Lat.	Lon.	Entity name	Reference (s)
Arch cave	660	50.55	-127.07	DM05-01	Marshall et al. (2009)
Beatus cave	875	46.38	7.49	EXC3, EXC4	Boch et al. (2011)
Bribin cave	500	-8.05	110.633	JB2	Hartmann et al. (2013)
Cesare Battisti cave	1880	46.08	11.02	CB25, CB39, CB47	Johnston et al. (2018)
Chan Hol cave	-8.5	20.16	-87.57	CH-7	Stinnesbeck et al. (2017)
Chen Ha cave	550	16.6769	-89.0925	CH04-02	Pollock et al. (2016)
Cold Water cave	356	43.4678	-91.975	CWC-1s, CWC-2ss, CWC-3l	Denniston et al. (1999)
Devil's Icebox cave	250	38.15	-92.05	DIB-1, DIB-2	Denniston et al. (2007b)
Dongge cave	680	25.2833	108.0833	DA_2005, D4_2005	Dykoski et al. (2005); Wang et al. (2005)
Dos Anas cave	120	22.38	-83.97	CG	Fensterer et al. (2010); Fensterer et al. (2012)
El Condor cave	860	-5.93	-77.3	ELC_composite	Cheng et al. (2013)
Frasassi cave system - Grotta Grande del Vento	257	43.4008	12.9619	FR16	Vanghi et al. (2018)
Goshute cave	2000	40.0333	-114.783	GC_2, GC_3	Denniston et al. (2007a)
Harrison's cave	300	13.2	-59.6	HC-1	Mangini et al. (2007); Mickler et al. (2004); Mickler et al. (2006)
Hoti cave	800	23.0833	57.35	H14	Cheng et al. (2009);Fleitmann et al. (2003)
Jaraguá cave	570	-21.083	-56.583	JAR4, JAR1, JAR_composite	Novello et al. (2017); Novello et al. (2018)
Karaca cave	1536	40.5443	39.4029	K1	Rowe et al. (2012)
Klaus Cramer cave	1964	47.26	9.52	KC1	Boch et al. (2011)
KNI-51 cave	100	-15.18	128.37	KNI-51-A1, KNI-51-P	Denniston et al. (2013)
Korallgrottan cave	570	64.88	14.15	K1	Sundqvist et al. (2007)
Lianhua	455	29.48	109.53	A1	Cosford et al. (2008a)
Lynds cave	300	-41.58	146.25	Lynds_BCD	Xia et al. (2001)
Mawmluh cave	1160	25.2622	91.8817	MAW-0201	Myers et al. (2015)
McLean's cave	300	38.07	-120.42	ML2	Oster et al. (2014)
Minnetonka cave	2347	56.5833	-119.65	MC08-1	Lundeen et al. (2013)
Moondyne cave	100	-34.27	115.08	MND-S1	Treble et al. (2003); Treble et al. (2005); Fischer and Treble (2008); Nagra et al. (2017)
Paraiso cave	60	-4.0667	-55.45	Paraiso composite	Wang et al. (2017)
Peqiin cave	650	32.58	35.19	PEK_composite, PEK 6, PEK 9, PEK 10	Bar-Matthews et al. (2003)

Piani Eterni karst system	1893	46.16	11.99	MN1, GG1, IS1	Columbu et al. (2018)
Poleva cave	390	44.7144	21.7469	PP10	Constantin et al. (2007)
São Bernardo cave	631	-13.81	-46.35	SBE3	Novello et al. (2018)
São Matheus cave	631	-13.81	-46.35	SMT5	Novello et al. (2018)
Shatuca cave	1960	-5.7	-77.9	Sha-2, Sha-3, Sha-composite	Bustamante et al. (2016)
Sofular cave	440	41.42	31.93	So-17A, So-2	Badertscher et al. (2011) Fleitmann et al. (2009) Göktürk et al. (2011)
Soylegrotta cave	280	66	14	SG93	Lauritzen and Lundberg (1999)
Tangga cave	600	-0.36	100.76	TA12-2	Wurtzel et al. (2018)
Uluu-Too cave	1490	40.4	72.35	Uluu2	Wolff et al. (2017)
White moon cave	170	37	-122.183	WMC1	Oster et al. (2017)
Xiangshui cave	380	25.25	110.92	X3	Cosford et al. (2008b)
Xibalba cave	350	16.5	-89	GU-Xi-1	Winter et al. (2015)
Yaoba Don cave	420	28.8	109.83	YB	Cosford et al. (2008b)

Table 2: Number of SISALv1b speleothem records available for key time periods. Mid-Holocene (MH): 6±0.5 kyrs BP; Last Glacial Maximum (LGM): 21±1 kyrs BP. "kyrs BP" refers to thousand years before present, where present is 1950 CE.

Time period	**Number of speleothems (entities) and cave sites in both periods**
Modern (1961–1990 CE)	7358 entities (4759 sites)
PI (1835–1865 CE)	62 76 entities (51 62 sites)
Extended PI (1850–1990 CE)	10087 entities (6981 sites)
MH and PI	2118 entities (1720 sites)
MH and extended PI	364 entities (2932 sites)
MH and Last Millennium (LM, 850–1850 CE)	5148 entities (3841 sites)
LGM and PI	75 entities (57 sites)
LGM and extended PI	131 entities (102 sites)
LGM and Last Millennium (LM, 850–1850 CE)	142 entities (102 sites)
LGM and MH	202 entities (168 sites)

Figure S1: Speleothem samples for the period 1958-2013 CE converted to their drip-water equivalent using the fractionation factors from Grossman and Ku (1986; black dots) and Tremaine Tremaine et al. (2011; red dots). We use simulated mean annual temperature (MAT) for the years when samples are available for the conversion. Vertical lines indicate the offset thresholds for 0.1 and 0.3 ‰ with the former corresponding to the average isotope uncertainty in the SISAL database. Maximum offset occurs at low MAT and is 0.86 ‰.

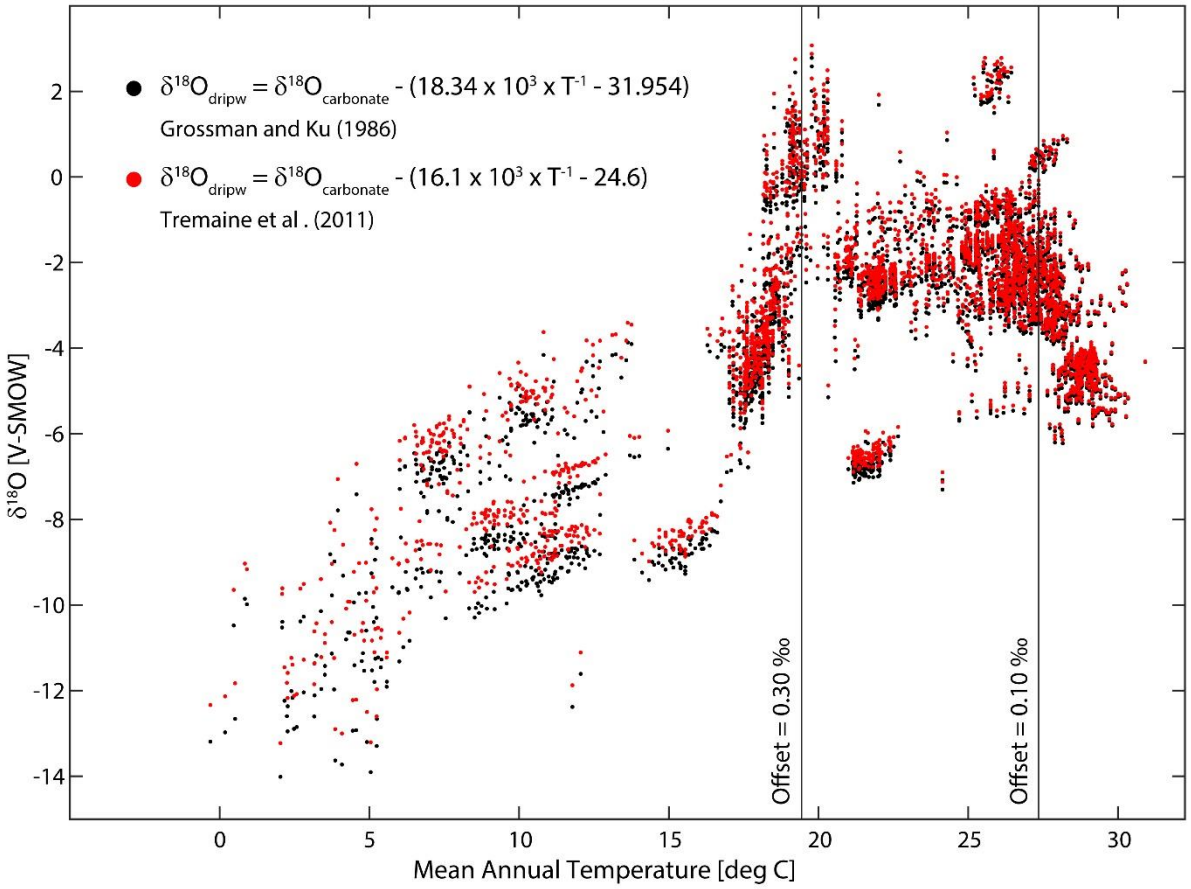

~~Supplementary~~ **Figure S~~1~~2:** Data-model comparison for the modern period (1958–2013) using three methods to treat the simulated data: **(a, b)** $\delta^{18}O$ in precipitation weighted according to the monthly precipitation amount. **(c, d)** $\delta^{18}O$ in precipitation weighted according to the monthly potential infiltration calculated as precipitation (P) minus evapotranspiration (E) when P-E > 0. **(e, f)** soil water $\delta^{18}O$ weighted according to the monthly soil moisture content (i.e. soil water bucket). (a, c, e) show the data-model agreement. (b, d, f) show the linear regressions of simulated $\delta^{18}O$ vs SISAL $\delta^{18}O$ data.

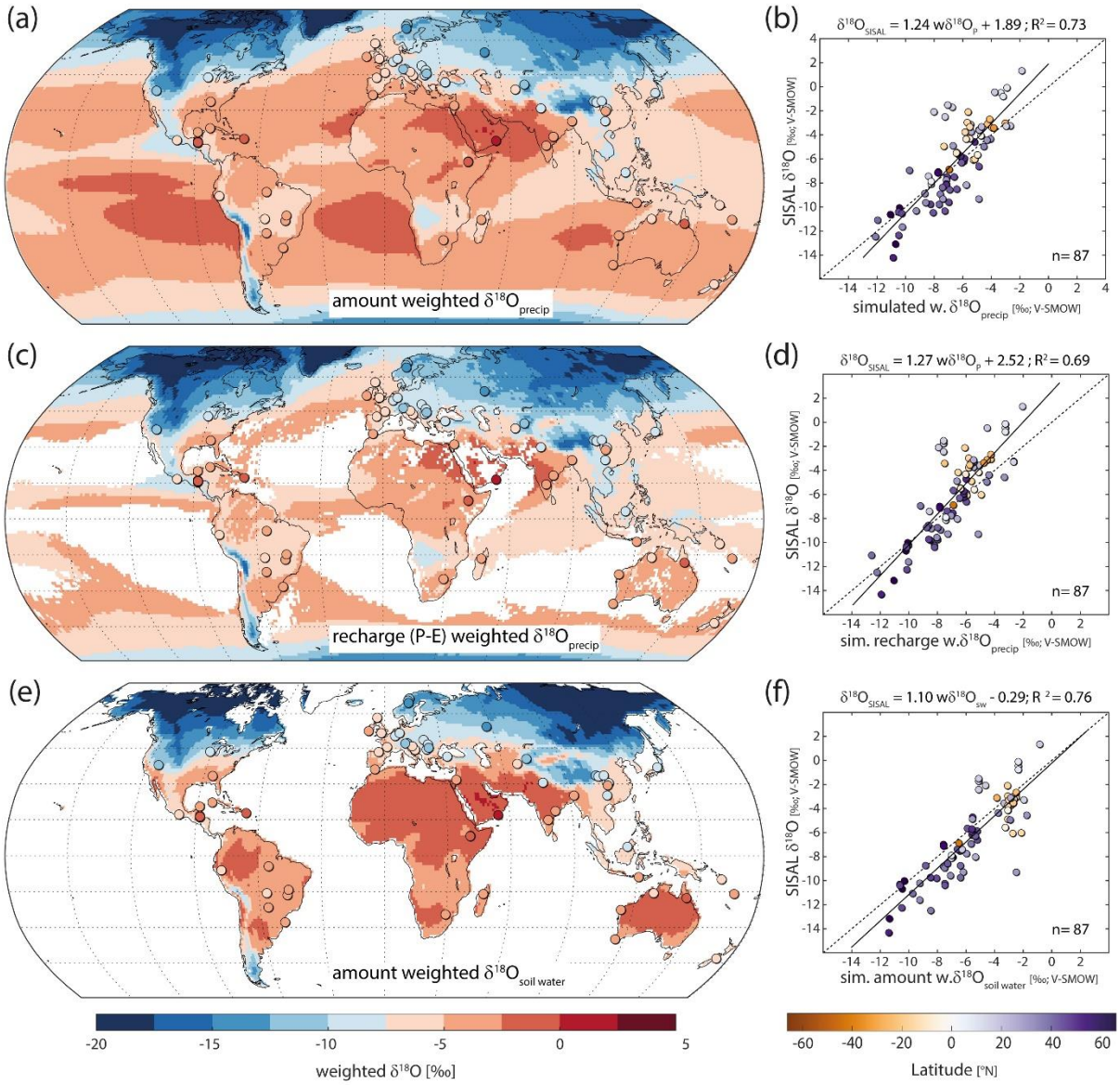

~~Supplementary~~ **Figure S3**: Linear regressions between SISAL $\delta^{18}O$ and simulated amount-weighted $\delta^{18}O$precip (top row), recharge weighted $\delta^{18}O$ (middle row) and amount weighted $\delta^{18}O$sw for the period (1958–2013 CE). Data used in first column are long-term SISAL and ECHAM5-wiso data (as in Supplementary Figure 1). Second column is the regression on a year to year basis (i.e. using simulated data only for the years for which SISAL data is available). Third, fourth and fifth columns are the same as the latter after applying a smoothing of 5- 10- and 15-yrs respectively. The smoothing was applied using the 5, 10 and 15 years previous to the SISAL's sample date and all years carried the same weight on the mean value. Solid black line is the regression line. Dashed grey line is the 1:1 line. Correlation coefficients (R^2) are at the bottom right of each panel.

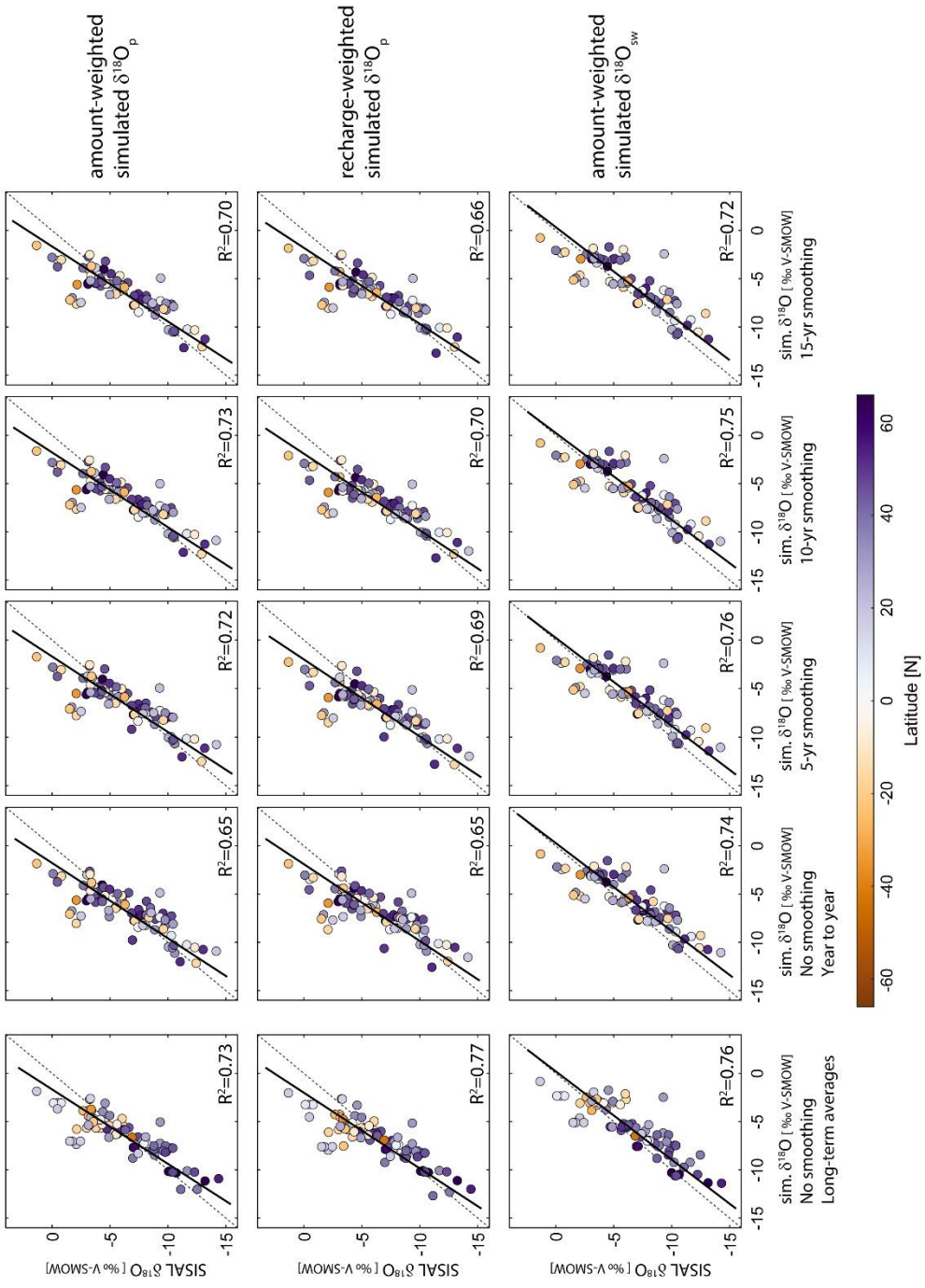

~~Supplementary~~ **Figure S~~3~~4:** Linear regression between SISAL $\delta^{18}O$ averages during the modern period (1961-1990 CE) and the pre-industrial (1850±15 CE). Colour bar shows the difference between the two time periods in ‰ V-PDB.

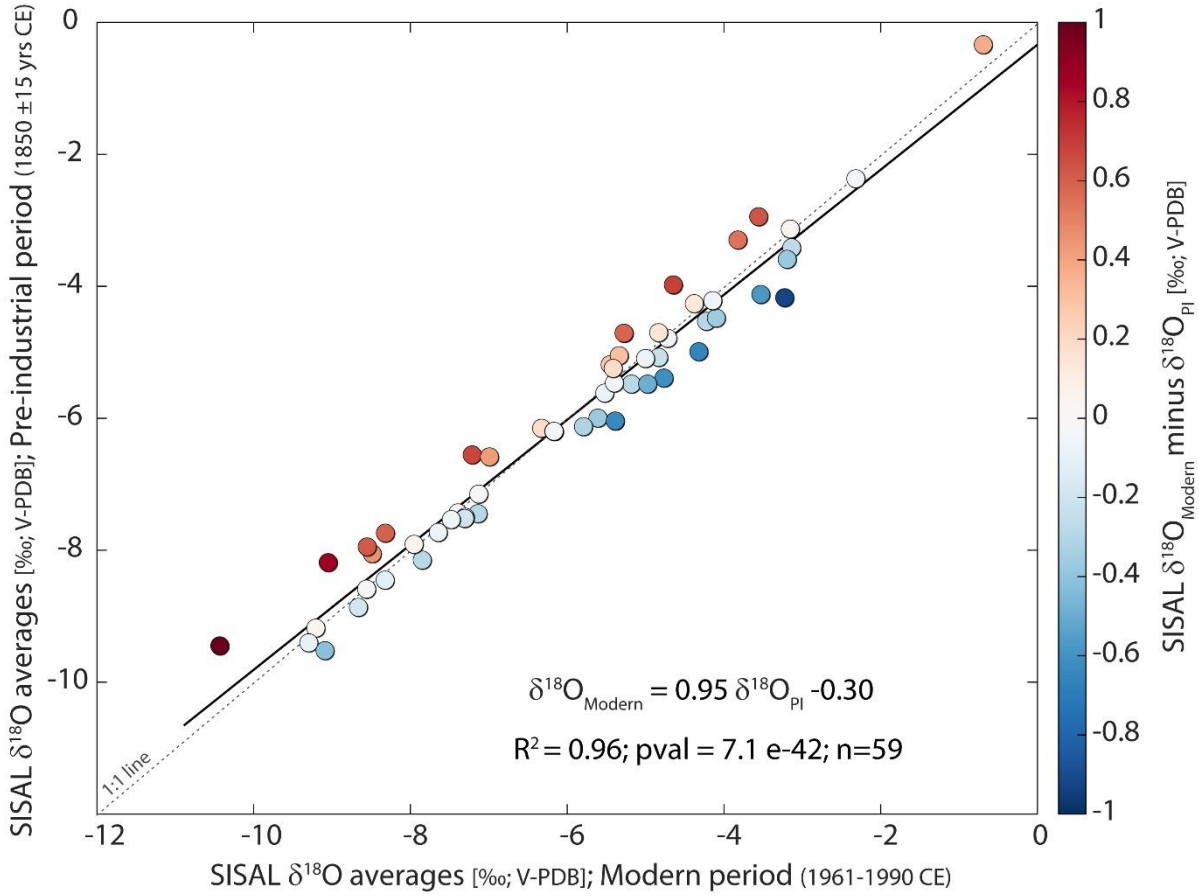

~~Supplementary~~ **Figure S45:** Impact of using time-windows shorter than the convention of ± 500 yrs on SISAL MH-PI anomalies. **(a)** Boxplots of the global $\delta^{18}O$ MH-PI anomalies across time window widths. **(b)** Anomalies using windows of 100 to 400 yrs versus the anomalies calculated using the conventional 500 yrs. **(c)** Differences between MH-PI anomalies using 500 and 100 yrs. See Supplementary Table 1 for the number of entities and sites available for each window width.

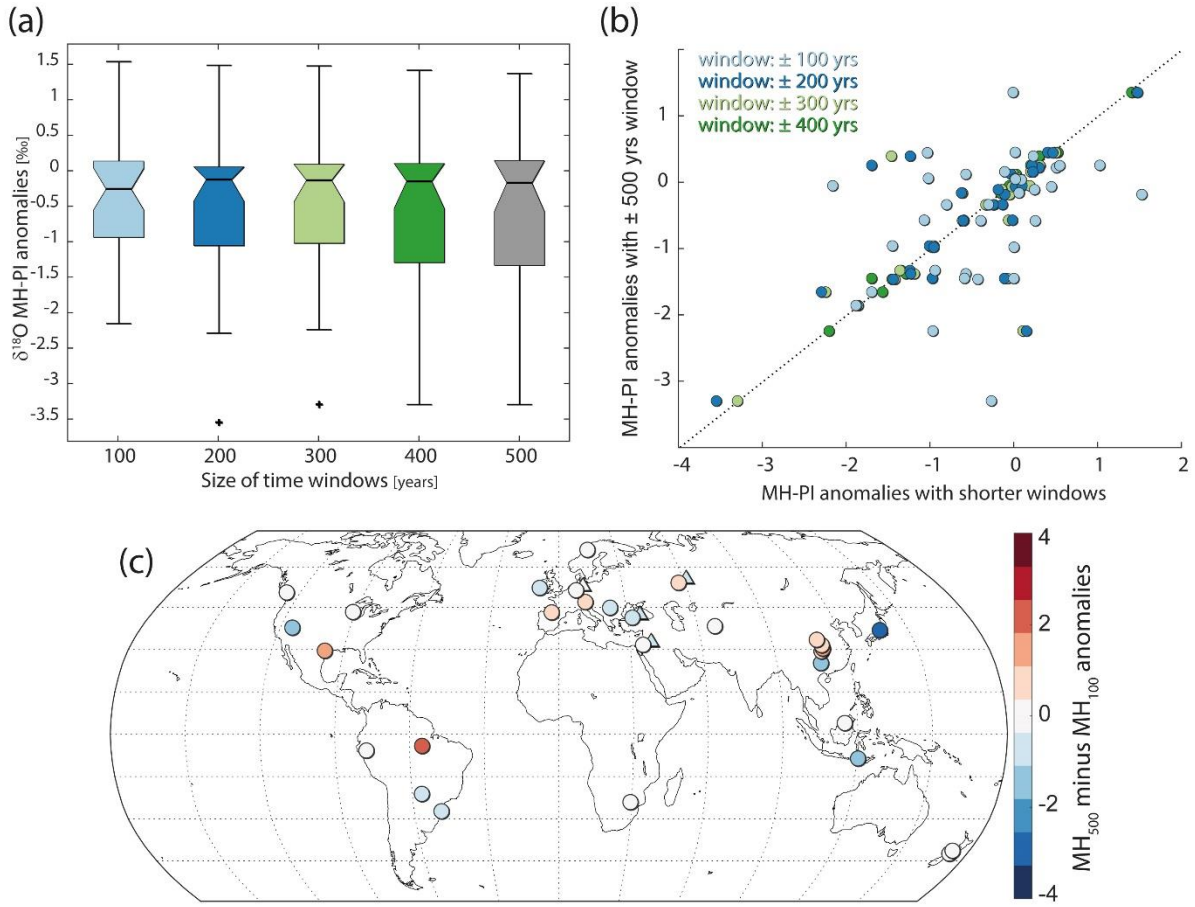

~~Supplementary~~ **Figure S~~5~~6:** Impact of using time-windows shorter than the convention of ± 1,000 yrs on SISAL LGM-PI anomalies. **(a)** Boxplots of the global $\delta^{18}O$ LGM-PI anomalies across time window widths. **(b)** Anomalies using windows of 200 to 400 yrs versus the anomalies calculated using the conventional 1,000 yrs. **(c)** Differences between LGM-PI anomalies using 1,000 and 200 yrs. See Supplementary Table 2 for the number of entities and sites available for each window width.

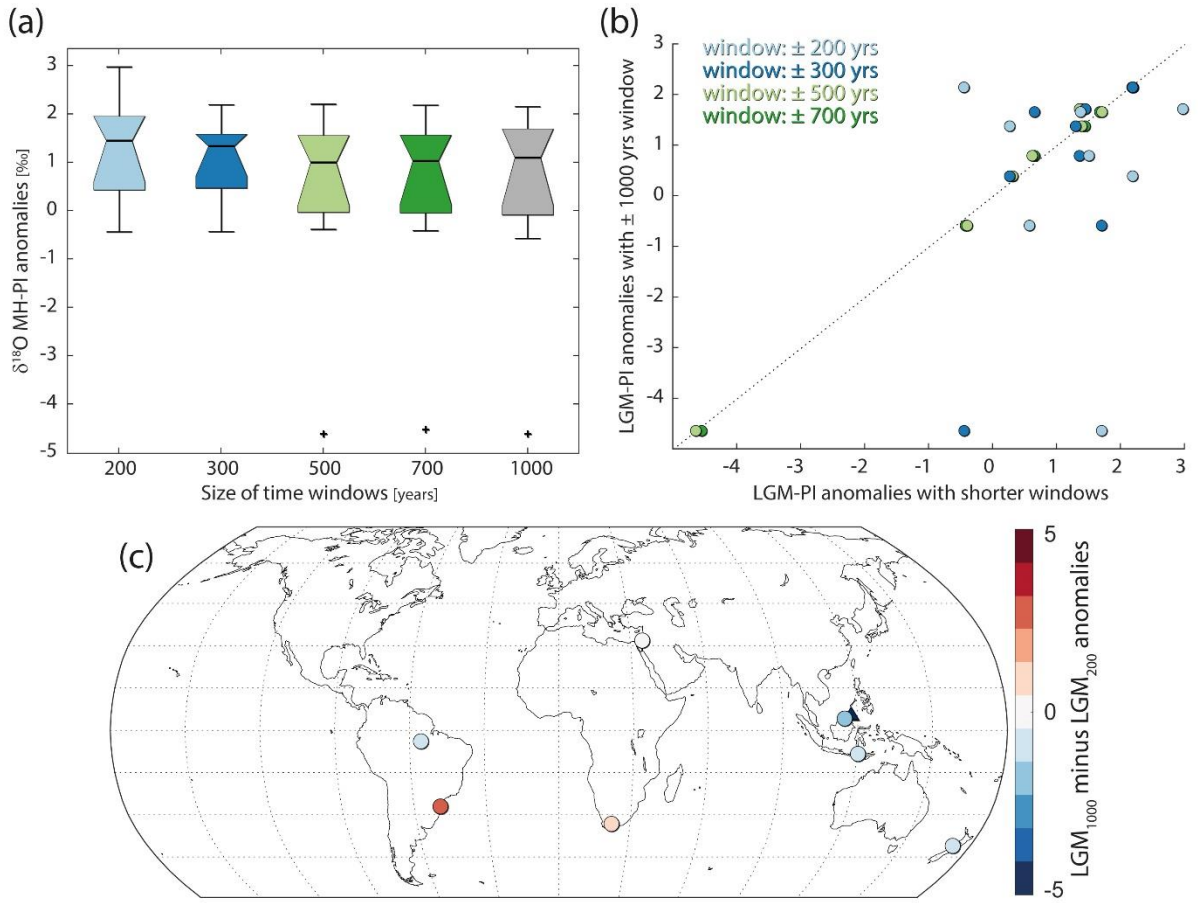

Table S1: Number of entities used in Supplementary Figure 5.

MH window size	Individual entities	Individual sites	Individual entities overlapping with ext. PI	Individual sites overlapping with ext. PI (1850-1990)
± 500 yrs BP	106	74	36	32
± 400 yrs BP	105	73	36	32
± 300 yrs BP	104	73	35	32
± 200 yrs BP	99	73	35	32
± 100 yrs BP	92	68	33	30

Table S2: Number of entities used in Supplementary Figure 6.

LGM window size	Individual entities	Individual sites	Individual entities overlapping with ext. PI	Individual sites overlapping with ext. PI
± 1000 yrs BP	48	35	11	10
± 700 yrs BP	45	34	10	10
± 500 yrs BP	43	33	10	10
± 300 yrs BP	41	31	9	9
± 200 yrs BP	39	29	8	8

Supplementary Section: Multivariate analysis

Methods:

Univariate multilinear analyses were applied on both speleothem and simulated $\delta^{18}O$ data for the three time periods (i.e. modern, MH and LGM). The analyses consisted in exploring the data to verify the statistical premises of a linear relationship between the variables, and if verified, selecting the best multilinear model based on a step-wise selection between the most complete linear regression model (e.g. see equation below) and the simplest one (e.g. $\delta^{18}O_y = constant$). In all univariate multilinear models, the dependent variable was $\delta^{18}O$ and the independent variables would include the $\delta^{18}O$ either from another data source (SISAL, OIPC, ECHAM5-wiso) and the same time period (modern, MH, LGM), or from another time period but the same data source. The analyses were made using the R software (R Core Team, 2015) following Zuur et al. (2010) scripts. The general equation of the applied model can be expressed as:

$$\delta^{18}O_y = a + b \cdot \delta^{18}O_x + c_t \cdot (lat \cdot lon \cdot elevation) + \varepsilon_t$$

Where y and x refer to the two data sources used (in ‰ V-SMOW); a, b and c_t are the coefficients of each independent variable and their interaction, respectively, and ε_t are the residuals. Longitude and latitude are expressed as degrees N and E, respectively, and elevation is in meters above sea level. The elevation in ECHAM5-wiso was used for MH and LGM time periods whereas SISAL elevation was used for the modern.

Results:

Our multivariate analysis shows that incorporating variables other than SISAL's $\delta^{18}O$ and simulated w$\delta^{18}O$p in the comparison (e.g. a parameter to account for latitudinal changes) does not improve the results from the simple linear regression in Figure 3. Nevertheless, our best multivariate linear model for the modern period includes the latitude as a significant variable for explaining, for example, the linear SISAL-ECHAM relationship in the modern period. This indicates that the geographical position of the samples has to be taken into account in order to better capture the linear relationship between the modern SISAL values and the modern ECHAM5-wiso experiments.

Supplementary Table 1: Results of the best multivariate linear regression models. Superindices are the statistical significance of the coefficients as ([a]) p-val < 0.01, ([b]) 0.01 < p-value < 0.05 and ([c]) 0.05 < p-value < 0.1. n is the number of observations for each model and R^2 is the correlation coefficient (either adjusted or not). $: Elevation was removed from the original complete model because it increases the Variance Inflation Factor (VIF) to values higher than 10. The combinations not in this table (e.g. ECHAM5-wiso MH vs LGM or ECHAM5-wiso LGM vs modern) did not yield any significant correlation.

y	**OIPC**	**ECHAM5-wiso mod**	**SISAL MH**	**SISAL LGM**	**ECHAM5-wiso LGM**
x	**SISAL mod**	**SISAL mod**	**SISAL mod**	**SISAL MH**	**ECHAM5-wiso MH**
intercept	0.463	-3.357 [a]	-1.197 [a]	1.43	0.786 [a]
d18O (x)	0.93 [a]	0.623 [a]	9.29 E-1 [a]	1.006 [a]	0.883 [a]
Latitude	-0.007	0.013 [b]	1.12 E-2	-0.064 [b]	-0.050 [a]
Longitude	-0.003	0.0031	-2.18 E-3	-0.003	0.001
Elevation	-1.81 E-4 c	$	$	$	$
Interaction lat*lon			-2.20 E-4 a	4.04 E-4	3.69 E-4 a
Interaction lon*elev					
R2 (adjusted)	0.81 (0.79)	0.78(0.77)	0.92 (0.91)	0.83 (0.78)	0.84(0.80)
n	66	72	28	20	20

Reference list

Grossman, E. L., and Ku, T.-L.: Oxygen and carbon isotope fractionation in biogenic aragonite: Temperature effects, Chemical Geology: Isotope Geoscience section, 59, 59-74, https://doi.org/10.1016/0168-9622(86)90057-6, 1986.

R: A Language and Environment for Statistical Computing, R Foundation for Statistical Computing: http://www.R-project.org, 2015.

Tremaine, D. M., Froelich, P. N., and Wang, Y.: Speleothem calcite farmed in situ: Modern calibration of δ18O and δ13C paleoclimate proxies in a continuously-monitored natural cave system, Geochimica et Cosmochimica Acta, 75, 4929-4950, https://doi.org/10.1016/j.gca.2011.06.005, 2011.

Zuur, A. F., Ieno, E. N., and Elphick, C. S.: A protocol for data exploration to avoid common statistical problems, Methods in Ecology and Evolution, 1, 3-14, https://doi.org/10.1111/j.2041-210X.2009.00001.x, 2010.